Elsevier Editorial System(tm) for Earth-Science Reviews

Manuscript Draft

Manuscript Number:

Title: Major dust events in Europe during marine isotope stage 5 (130-74 ka): A climatic interpretation of the "markers"

Article Type: Review Article

Keywords: dust events, last climate cycle, abrupt changes, Dolni Vestonice loess sequence, blocking pattern, polar outbreaks

Corresponding Author: Dr. Denis-Didier Rousseau,

Corresponding Author's Institution: Ecole Normale Supérieure

First Author: Denis-Didier Rousseau

Order of Authors: Denis-Didier Rousseau; Michael Ghil; George Kukla; Adriana Sima; Pierre Antoine; Markus Fuchs; Christine Hatte; France Lagroix; Maxime Debret; Olivier Moine

Abstract: At present, major dust storms are occurring at mid-latitudes in the Middle East and Asia, as well as at low latitudes in Northern Africa and in Australia. Western Europe, though, does not experience such dramatic climate events, except for some African dust reaching it from the Sahara. This modern situation is of particular interest, in the context of future climate projections, since the present interglacial is usually interpreted, in this context, as an analog of the warm Eemian interval. European terrestrial records show, however, major dust events during the penultimate interglacial and early glacial. These events are easily observed in loess records by their whitish-color deposits, which lie above and below dark chernozem paleosols in Central European records of Marine Isotope Stage (MIS) 5 age.

We describe here the base of the Dolni Vestonice (DV) loess sequence, Czech Republic, as the reference of such records. The dust is deposited during intervals that are characterized by poor vegetation — manifested by high δ13C values and low magnetic susceptibility — while the fine sand and clay in the deposits shows grain sizes that are clearly different from the overlying pleniglacial loess deposits. Some of these dust events have been previously described as "Markers" or Marker Silts (MS) by one of us (G. Kukla), and are dated at about 111-109 ka and 93-92 ka, with a third and last one slightly visible at about 75-73 ka. Other events correspond to the loess material of Kukla's cycles, and are described as eolian silts (ES); they are observed in the same DV sequence and are dated at about 106-105 ka, 88-86 ka, and 78.5-77 ka.

The fine eolian deposits mentioned above, MS as well as ES, correspond to short events that lasted about 2 ka; they are synchronous with re-advances of the polar front over the North Atlantic, as observed in marine sediment cores. These deposits also correlate with important changes observed in European vegetation. Some ES and MS events appear to

be coeval with significant dust peaks recorded in the Greenland ice cores, while others are not. This decoupling between the European eolian and Greenland dust depositions is of considerable interest, as it differs from the fully glacial situation, in which the Eurasian loess sedimentation mimics the Greenland dust record. Previous field observations supported an interpretation of MS events as caused by continental dust storms. We show here, by a comparison with speleothems of the same age found in the northern Alps, that different atmospheric-circulation modes seem to be responsible for the two categories of dust events, MS vs. ES.

Suggested Reviewers: Dan Muhs
dmuhs@usgs.gov
Among the world leaders in dust and paleodust studies

Nathalie Mahowald
mahowald@cornell.edu
World expert in modeling climate and dust cycle in both present and past times

Gisela Winckler
winckler@ldeo.columbia.edu
Word expert in paleodust studies in marine cores

Hubertus Fischer
hubertus.fischer@climate.unibe.ch
World expert in dust studies in ice-cores

Opposed Reviewers: Slobodan Markovic
Serbian scientist having a conflict of interest with the submitting group

Ian Smalley
Conflict of interest with the authors

Cover letter

LABORATOIRE DE METEOROLOGIE DYNAMIQUE

UMR 8539 – ECOLE NORMALE SUPERIEURE– 24 RUE LHOMOND
75231 PARIS Cedex 05 (FRANCE)
Dr. Denis-Didier ROUSSEAU (rousseau@lmd.ens.fr)
Tel. 33 (0)1 44 32 27 24 Fax: +33 (0)14432 2727
Secrétariat : +33 (0)1 44 32 22 21 Fax: +33 (0)1 43 36 83 92
Site Web : http ://www.lmd.jussieu.fr/

Earth-Sci Reviews editors
Paris 25/9/2012

Dear colleagues,

Please find the paper we are submitting to Earth-Science Reviews which corresponds to a multidisciplinary investigation of the famous Dolni Vestonice that we revisited in 2009 with permission of the Czech authorities, as this site is a strictly protected one.

The paper we submit is mostly focussing on the bottom of the record, covering the base of the last climate cycle in which are recorded particular dust events. These dust events were first described long time ago by George Kukla in the 60s but no precise interpretation has been given beside the possible result of "continental duststorms".

Thanks to the multidisciplinary investigation performed on this sequence, we were able to characterize these eolian deposits described within 2 soil complexes covering the interval 130-74 ka. The availability of new OSL dates provided us the opportunity to propose correlation with other climate events recorded Europewide but also in North Atlantic marine cores as well as in Greenland ice-cores. Finaly, refering to present meteorological mechanisms, we are proposing some climatic mechanism to interpret the occurrence of these particular dust events over Europe.

We therefore consider that the paper, in its present form, is of great interest for Earth-Science Reviews readers. Moreover, as part of a national grant of the French funding agency, this study is a follow up of previous papers published in QSR like Rousseau et al 2002, Antoine et al, 2009, Sima et al, 2009 among others.

Looking forward to reading from you
All the very best

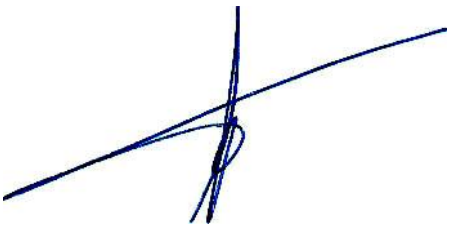

denis-didier Rousseau

*Manuscript
Click here to download Manuscript: Dust_markers_def25092012.docx Click here to view linked References

Major dust events in Europe during marine isotope stage 5 (130–74 ka): A climatic interpretation of the "markers"

Denis-Didier Rousseau[a,b], Michael Ghil[a,c], George Kukla[b], Adriana Sima[a], Pierre Antoine[d], Markus Fuchs[e], Christine Hatté[f], France Lagroix[g], Maxime Debret[a], Olivier Moine[d]

[a] Ecole Normale Supérieure, Laboratoire de Météorologie Dynamique, UMR CNRS 8539, & CERES-ERTI, 24 rue Lhomond, 75231 Paris cedex 05, France

[b] Lamont-Doherty Earth Observatory of Columbia University, Palisades, NY 10964, USA

[c] Department of Atmospheric and Oceanic Sciences, University of California, Los Angeles, CA 90095-1565, & Institute of Geophysics and Planetary Physics, University of California, Los Angeles, CA 90095-1567, USA

[d] Laboratoire de Géographie Physique, UMR CNRS 8591, 1 place Aristide Briand, 92195 Meudon, France

[e] Department of Geography, Justus-Liebig-University Giessen, 35390 Giessen, Germany

[f] Laboratoire des Sciences du Climat et de l'Environement, UMR CEA-CNRS-UVSQ 8212, Domaine du CNRS, 91198 Gif-sur-Yvette, France

[g] Institut de Physique du Globe de Paris, Sorbonne Paris Cité, University Paris Diderot, UMR 7154 CNRS, 75005 Paris

Corresponding author: Denis-Didier Rousseau, denis.rousseau@lmd.ens.fr

ABSTRACT

At present, major dust storms are occurring at mid-latitudes in the Middle East and Asia, as well as at low latitudes in Northern Africa and in Australia. Western Europe, though, does not experience such dramatic climate events, except for some African dust reaching it from the Sahara. This modern situation is of particular interest, in the context of future climate projections, since the present interglacial is usually interpreted, in this context, as an analog of the warm Eemian interval. European terrestrial records show, however, major dust events during the penultimate interglacial and early glacial. These events are easily observed in loess records by their whitish-color deposits, which lie above and below dark chernozem paleosols in Central European records of Marine Isotope Stage (MIS) 5 age.

We describe here the base of the Dolni Vestonice (DV) loess sequence, Czech Republic, as the reference of such records. The dust is deposited during intervals that are characterized by poor vegetation — manifested by high $\delta^{13}C$ values and low magnetic susceptibility — while the fine sand and clay in the deposits shows grain sizes that are clearly different from the overlying pleniglacial loess deposits. Some of these dust events have been previously described as “Markers” or Marker Silts (MS) by one of us (G. Kukla), and are dated at about 111–109 ka and 93–92 ka, with a third and last one slightly visible at about 75–73 ka. Other events correspond to the loess material of Kukla’s cycles, and are described as eolian silts (ES); they are observed in the same DV sequence and are dated at about 106–105 ka, 88–86 ka, and 78.5–77 ka.

The fine eolian deposits mentioned above, MS as well as ES, correspond to short events that lasted about 2 ka; they are synchronous with re-advances of the polar front over the North Atlantic, as observed in marine sediment cores. These deposits also correlate with important changes observed in European vegetation. Some ES and MS events appear to be coeval with significant dust peaks recorded in the Greenland ice cores, while others are not. This decoupling between the European eolian and Greenland dust depositions is of considerable interest, as it differs from the fully glacial situation, in which the Eurasian loess sedimentation mimics the

Greenland dust record. Previous field observations supported an interpretation of MS events as caused by continental dust storms. We show here, by a comparison with speleothems of the same age found in the northern Alps, that different atmospheric-circulation modes seem to be responsible for the two categories of dust events, MS vs. ES.

Keywords: dust events, last climate cycle, abrupt changes, Dolni Vestonice loess sequence, blocking pattern, polar outbreaks

1. Introduction

Investigations of past dust deposits referred so far to glacial periods, during which fine grained material was supposed to be mobilized and transported by a modified atmospheric circulation constrained by the occurrence of continental ice sheets and sea level lowering. The modern-era situation, though, does not seem to have an obvious analog in the past, considering that Greenland ice cores show a difference in grain size between the dust deposited during glacial intervals —such as marine isotope stages (MIS) 4, 3 and 2 — and interglacial intervals sensu lato, such as MIS 5 (Ruth, et al., 2003). Evidence from marine cores shows that the contribution of the present African (Stuut, et al., 2005), Asian (Tada, et al., 1999), and Australian (Hesse and McTainsh, 2003) deserts was important in the past as well; therefore, physical parameter values required for present dust emission in these areas should still be of use. Transport and deposition rates, however, must have evidently changed because of the different environmental conditions.

In mid-latitudes, paleo-dust material originated mostly from dry riverbeds and emerged areas on the continental shelf, i.e. from regions that do not yield nowadays any dust. These regions were nevertheless particularly active and favored the deposition of mid-latitude loess sequences in the Northern Hemisphere.

Investigating atmospheric dustiness during interglacial intervals appears therefore even more challenging because of limitations in the resolution and completeness of ice core records, especially in the Northern Hemisphere. (GRIP members, 1993) described brief dust events in the Greenland GRIP ice core at 131 and 115 kyrs BP, which they named events 2 and 1, respectively, and interpreted them as being of very short duration (750 and 70 years). (Chappellaz, et al., 1997), however, used CH_4 analyses to challenge some of these claims, and showed that these dust events corresponded to older ice layers injected into the record.

In this paper, we describe several dust event records observed during MIS 5 in terrestrial deposits, and provide an interpretation thereof from a climate dynamics point of view. The next

85 section contains the description of the loess sequences, and the following one their climatic
86 interpretation. A short conclusion section rounds off the paper.
87
88
89 ## 2. Paleodust records of the last climate cycle
90
91 ### 2.1. Glacial Interval
92
93 #### 2.1.1. The Greenland ice cores
94 Several ice cores drilled at the summit of the Greenland ice sheet show a highly variable climate
95 during the last climatic cycle, with abrupt warmings followed by a two-step cooling towards
96 stadial conditions. The location of these cores is shown in Fig. 1.
97 Both the GRIP and GISP2 records present similar features, such as the parallelism
98 between the distinct $\delta^{18}O$ curves since about 110 ka (Dansgaard, et al., 1993). The good
99 correlation with the NorthGRIP record (Andersen, et al., 2004) increases further the reliability
100 of these earlier records. Rapid climate variations are also recorded in high-resolution marine
101 cores from the North Atlantic (Bond and Lotti, 1995). So-called Dansgaard-Oeschger (D/O)
102 events (Dansgaard and Oeschger, 1989, Dansgaard, et al., 1993) had been recognized in several
103 older Greenland ice cores — see Camp Century and Dye 3 curves (Dansgaard, et al., 1982) —
104 but were not widely accepted, especially when compared with lower resolution marine cores
105 (Dansggard, et al., 1985)
106 The dust record in these ice cores also shows variations that follow roughly the D/O
107 pattern, as the stadial intervals always reveal the occurrence of high dust content in the
108 atmosphere, contrary to low dust concentrations during the interstadials (Dansgaard, et al.,
109 1993, Hammer, et al., 1985) (Fig. 1). Some of the dust-record oscillations were linked with the
110 iceberg-discharge dynamics corresponding to the Heinrich events (Bond, et al., 1992, Heinrich,
111 1988), but are not evidently marked in the isotopic ice-core records.

112

113 2.1.2. Loess sequences

114 Loess is mostly an eolian sediment, which generally presents material of local, as well as more
115 regional or dispersed origin (Kukla, 1977, Pécsi, 1990). It corresponds to particular
116 environmental conditions, which made the fine material available — mainly from sandurs or
117 dried braided rivers, moraines, or even emerged landscapes after the lowering of the sea level
118 — and transported this material by strong winds. Considering the loess distribution, the
119 thickness of the sequences, and their eolian origin, loess series are a particularly good
120 continental record of past climates.

121 During the past decade, new techniques and study protocols have facilitated the use of
122 loess sequences as a sensitive tool to understand past climate dynamics. These techniques
123 include geophysical ones, such as magnetic susceptibility (Heller, et al., 1991, Kukla, et al.,
124 1988), geochemical ones, such as the analysis of stable isotopes (Gu, et al., 1991), as well as
125 biological indices (Lu, et al., 1991, Rousseau and Puisségur, 1990, Rousseau, et al., 1990,
126 Rousseau, 1991, Rousseau and Kukla, 1994, Rousseau and Wu, 1997, Wu, et al., 1995)
127 Detailed stratigraphic investigations remain, however, a fundamental tool that is still as
128 important as the more recent and sophisticated approaches.

129 Chinese loess sequences have been intensively studied by now for their climatic properties
130 (Ding, et al., 1992, Guo, et al., 1996, Heller and Liu, 1982, Kukla, 1987, Liu and collaborators,
131 1985). These sequences show the alternation of paleosol and loess units down to the Quaternary
132 boundary at 2.6 Myrs, and have recently been expanded to the Tertiary, down to 22 Myrs (Guo,
133 et al., 2002). The most widespread approaches in their investigation are the study of grain size
134 variations and the analysis of the low magnetic susceptibility hypothesized by Kukla et al.
135 (1988) as a record of the dust input. While Kukla's interpretation of dust deposition was
136 criticized for the soil intervals, because of the partly biological origin of the magnetic grains
137 (Heller, et al., 1991), the variation in grain size was used to infer climatic effects linked to the
138 Southeast Asian paleo-monsoon, as well as to North Atlantic variations (Porter and An, 1995).

Focusing on the last climate cycle, several superimposed soils have been described within the S1 soil complex, which is equivalent to marine MIS 5; some records, located in the northwestern part of the loess plateau, do exhibit the occurrence of loess or eolian layers (An, et al., 1991) named S1-2 and S1-4 (Ding, et al., 1999). Except for these rare locations, the general stratigraphy of the Chinese loess plateau does not indicate, however, any major dust input during MIS 5. Forster and Heller (1994), Ding et al. (2002) and Shackleton et al. (1995) indicated that, according to magnetic-susceptibility studies, the loess stratigraphy in Tajikistan is almost the same as in China. Kukla and colleagues (Smiley, et al., 1991) also proposed wider correlations between China, Central Europe and North America by considering the loess-paleosol successions that show a more global pattern in the general loess stratigraphy. In fact, while in China and Tajikistan — and, to some extent, in the Great Plains of North America — the loess sequences corresponds mostly to tabular deposits, building through time a plateau-like structure, the European loess sequences are often deposited on slopes. In that case the sequences are not only a succession of paleosols and loess, like in Asia; instead, they are a succession of soil complexes and loess.

Numerous stratigraphers have also intensively studied and carefully described European loess sequences; the location of the major sequences is plotted in Fig. 2. Kukla (1961) and Kukla and Lozek (1961) were the first to define a typical stratigraphic sequence for Europe. Their succession is based on cycles and it varies somewhat according to the region considered. Each cycle starts by a thin deposit of hillwash loam, called phase 1. A forest soil of braunerde type (phase 2) follows, covered in turn by a steppe soil of chernozem type (phase 3). An eolian deposit of small thickness, named Marker (phase 4), interrupts this steppe soil, and it is further overlaid by bedded layers of pellet sands or Lehmbröckelsände (phase 5) and finally a loess layer. Marker units are thin bands of fine-grained silt that separate underlying black humiferous steppe soil from overlying pellet sands; hereafter we will refer to these units as Marker silts (MS). Such cycles can repeat through time, more or less completely.

Investigating the loess member of this cyclic succession, Rousseau and coworkers (2002, 2007) showed that European sequences — located at the winter margin of sea ice extension, at a latitude of about 50° N, where they are the thickest on average (Fig. 2) — recorded doublets that correspond to successive alternations of paleosols and loess or eolian units. This team of researchers has constrained the cyclic successions well by different dating methods (Hatté, et al., 1999, Lang, et al., 2003) and it has successfully correlated them with climate variations that represent alternations of warm interstadial D/O events and cold stadial intervals, recorded in Greenland ice cores and North Atlantic marine-sediment cores (Antoine, et al., 2009).

Rousseau et al. (2011) have provided further evidence of this correlation by showing that the type of paleosol preserved in the continental sequences corresponds directly to the duration of the interstadial preserved in ice and marine cores. This alternating sequence lies over a pedocomplex subsequence showing also a complex succession, which corresponds to previously well-expressed cycles of hillwash loam, paleosol-organic soil, MS, pellet sands, and seolian deposits, as described by Kukla and Lozek (1961). The work performed over the last decade showed, however, that the completeness of the sedimentary cycles corresponds to precise climatic conditions, rather than occurring at random, as originally supposed by Kukla and Lozek (1961).

These observations in terrestrial records could lead one to interpret the variations in the atmospheric dust content recorded in Greenland during MIS 5 as minor climatic phenomena, compared to those of higher magnitude that had been described during MIS 4–2. The isotopic signature of Greenland dust shows similarities with Chinese loess (Biscaye, et al., 1997, Svensson, et al., 2000), and present dust deposited in Greenland firn exhibits also a Chinese origin, mostly from the northern deserts (Bory, et al., 2002). Even though the dust deposition recorded in the Greenland ice sheet during MIS 5 is of lower magnitude than during full glacial times, it would appear that major dust emissions, compared to the present, should have occurred in the deserts of Northern China. This line of reasoning appears to imply favorable environmental conditions for dust emission and transport from these deserts. Considering the

192 tight relationship described between Greenland records and European loess series for the last
193 climate cycle, could such a relationship have also been active during MIS 5? If not, can one or
194 more other mechanisms be proposed?
195
196 ## 2.2. MIS 5 dust record
197
198 ### 2.2.1) The Greenland ice core GRIP
199 The record of major dust events prior to the last glacial time in Greenland ice cores is less well
200 covered in the existing literature. Indeed, from 120 kyr upward, three dust peaks have been
201 reported (Andersen, et al., 2004, GRIP members, 1993); they seem to occur just before the
202 boundary between MIS 5 and 4, at about 74 ka (Fig. 1). These peaks correspond to coolings that
203 are well captured by the $\delta^{18}O$ curve at 111–98 ka, 89–85 ka, and 79–77 ka, respectively.
204 In the Southern Hemisphere, the dust content in the Vostok ice core does not show any
205 particular peak (Petit, et al., 1990), while both the EDML and EDC ice core records do show
206 dust peaks at about the same time interval as in Greenland (Fischer, et al., 2007). These peaks
207 are identified less clearly, however, than in the Greenland $\delta^{18}O$ and dust records. The
208 difference between the two groups of records indicates that the MIS 5 dust record in Greenland
209 ice cores points to a climate history associated with the Northern Hemisphere, rather than with
210 both hemispheres. Therefore, Northern Hemisphere atmospheric dynamics could have played an
211 important role in the extent to which some, if not all, of these events have been recorded in the
212 above-mentioned continental sequences, especially in the European loess sequences.
213
214 ### 2.2.2. Central European loess sequences
215 Kukla (1961) described three major pedocomplexes — PKIII, PKII and PKI — during the last
216 climatic cycle. In this by now classical interpretation of the Central European loess sequences,
217 the first two were assigned to MIS 5 (Fig. 3). Kukla (1977) noticed the occurrence of three

218 “marker units” in pedocomplexes PKIII and PKII, and interpreted them as corresponding to
219 paleo-dust intervals.

220 Fuchs et al. (2012) and Antoine et al. (submitted) provide further information about
221 these particular dust layers in the Dolni Vestonice (DV) section (Moravia, Czech Republic),
222 which was continuously sampled every 5 cm. First of all, the succession identified in the new
223 section is in total agreement with the previous description of the sequence by B. Klima and G.
224 Kukla in 1968, as published in (Demek and Kukla, 1969) and by Kukla (1977). A detailed field
225 investigation allowed Fuchs and colleagues (2012) to identify a complex succession of 22
226 pedosedimentary units for the last climate cycle (Fig. 3).

227 Based on these 22 units, their sedimentological characteristics and the occurrence of
228 well-developed soil horizons, erosion boundaries and facies changes, four subsequences (I to
229 IV) were distinguished, including the last interglacial paleosol, a Bt horizon (unit 21) to the
230 surface of the upper loess (unit 1), with the first sub-sequence corresponding to the basal humic
231 soil complex (units 20 to 9) including pedocomplexes PKIII and II. The basal subsequence
232 starts by the forest Bt paleosol (unit 21); a first chernozem (unit 19), labeled as isohumic soil
233 horizon (ISH) 1; a marker silt (unit 18, MS 1); pellet sands (Lehmbröckelsände, unit 17),
234 labeled as PS 1; and an eolian silt (unit 16, ES 2). This succession corresponds to Kukla’s
235 (1977) cyclic pattern and to the soil complex PK III. The succession repeats twice thereafter but
236 not completely, inasmuch as the Bt horizon is missing. Chernozem of unit 11 shows a more
237 complex evolution as a light layer divides it into two sub-units, the lowermost being more
238 developed than the upper one, a characteristic that G. Kukla had also described previously, cf.
239 Klima and Kukla (1968) in (Demek and Kukla, 1969) (Fig. 4).

240 The overlying subsequence II starts with a discontinuity between units 9 and 8. Unit 8 shows
241 the occurrence of a very distinct sandy component, with increasing fine sand contents from 23%
242 in unit 8 to 30% at the top of unit 7 (Fuchs, et al., 2012).

243 The multidisciplinary investigation of the DV sequence allows one to describe the variations
244 of several environmental parameters measured along the stratigraphy (Antoine et al.,

245 submitted); see Figs. 3 and 5 here. The interglacial paleosol indicates increasing clay content,
246 susceptibility values, total carbonate and negative values towards its top, all of these being
247 features characteristic of the Bt horizon. The chernozems ISH 2,3 show high clay content
248 (minimum 35%), high susceptibility values (minimum 45 m^3/kg), increasing carbonate towards
249 the top, and the more negative $\delta^{13}C$ values, at about –26‰, characteristic of C3 vegetation.
250 These analytic results (clay and total carbonate content, magnetic susceptibility, $\delta^{13}C$)
251 demonstrate that this unit 11 can be subdivided into two distinct subunits (ISH 3a & 3b), with
252 the lower soil horizon (ISH 3a) being more developed (Fig. 3, 5). Slight differences occur,
253 however, in ISH 4, which shows lower values of magnetic susceptibility, carbonate content, less
254 negative $\delta^{13}C$, and is not marked in the clay content.

255 The marker silts MS 1, 2 and 3 have low clay content, but not as low as the overlying loess
256 units. The magnetic susceptibility is low in MS 1, 2 and 3, but higher than in the chernozems
257 (ISH). The carbonate content in the marker silts is low (maximum 6-7%), but slightly higher
258 than in the chernozems, while the $\delta^{13}C$ indicates less negative values, of about –25‰. The
259 markers show a lower brightness (L* between 42% and 52%) and a low iron hydroxide content
260 (FDS 555 between 0.07 and 0.12) than the eolian silts. The exact definitions of the two
261 spectrometric parameters — sediment L* (in percentages) and FDS — are given in Debret et al.
262 (2011) and in the caption of Fig. 5.

263 The ES layers have low clay content, lower even than previously deposited marker silts. The
264 magnetic susceptibility is low, while the total carbonate content is higher than 15%. The $\delta^{13}C$
265 indicates more aridity with less negative values that are similar to those measured in the MS
266 layers.

267 Finally the pellet sands (PS) indicate intermediate values of various parameters between
268 those of the ISH and the MS. The carbonate content, at about 25.5 ‰, is higher than in ISH, but
269 lower than in ES or MS. The brightness and iron hydroxide content exhibit values of L* = 50–
270 55 % and FDS 555 between 0.1 and 0.13, which are intermediate between those that

271 characterize the marker silts and the proper loess unit above pedocomplex PKII; the latter are
272 given by L* > 60% and FDS 555 > 0.14.

273 The Optical Stimulated Luminescence (OSL) ages derived from different grain size
274 fractions, labeled BT in accordance with the Bayreuth luminescence lab (Fuchs, et al., 2012) are
275 the same within measured error limits, and all OSL age estimates are in the proper stratigraphic
276 order (Fuchs, et al., 2012). For the OSL dates, we consider the interval given by the measured
277 errors, which show that the stratigraphy of the DV sequence is in good agreement with the
278 $\delta^{18}O$ stratigraphy from NGRIP (Andersen, et al., 2004). The latter $\delta^{18}O$ stratigraphy is
279 supported in turn by the $\delta^{18}O$ stratigraphy obtained in the Chinese speleothems from the Hulu
280 and Sanbao caves (Wang, et al., 2008, Wang, et al., 2001), and in a recently published Northern
281 Alps record (Boch, et al., 2011), as shown in Figs. 6 and 7.

282 OSL sample BT 753 was taken from the homogeneous eolian silt of unit 18 (MS 1),
283 providing an age of 108.9 ± 6.82 ka. Therefore, the sediment was deposited during stage MIS
284 5d, and hence it represents the first eolian sediment of the Early Glacial. The first chernozem
285 horizon (unit 19, ISH 1) below this silt layer represents the oldest soil unit of the Weichselian
286 Early Glacial. Assigning numerical ages for the formation of this humic soil before roughly 110
287 ka is a first for European Early Glacial soil complexes. According to the $\delta^{18}O$ curve from North
288 GRIP (Andersen, et al., 2004), the humic soil of unit 19 can be assigned to the short Greenland
289 interstadial GIS 25 (~ 111–113 ka; cf. (Dansgaard, et al., 1993). This age assignment also
290 supports the age proposed by Kukla and Koci (1972) for the shift between the forest,
291 represented by chernozem unit 19, and the steppe, represented by MS1 unit 18; these authors
292 identified the forest-steppe shift with the lower boundary of the geomagnetic Blake event at
293 about 126 ka.

294 The eolian silt layer ES1 corresponds to unit 16 and it yields an OSL date of 104.93 ± 6.79
295 ka; assuming the completeness of the sequence, these dates correspond to Greenland stadial
296 GS23 (Rousseau, et al., 2006) (Fig. 7). The first Kukla cycle encompasses, therefore, the Last
297 Interglacial, as well as two Greenland stadials and interstadials.

Two other prominent chernozem soil horizons (unit 15, IHS 2, and unit 11, IHS 3a and 3b) are observed in the DV stratigraphy. Kukla's cyclic pattern partly occurs twice but in a truncated version (chernozem, marker silt, pellet sands, and eolian silt only), due to the lack of the Bt horizon. These soils correspond to temperate continental intervals, which could roughly be coeval with Greenland insterstadials. Indeed, the OSL sample taken from the upper part of the chernozem of unit 15 is dated to 90.25 ± 5.99 ka (BT 755) and thus could be correlated with GIS 23, which in turn corresponds to MIS 5c (Andersen, et al., 2004).

The OSL sample taken from the top of the following composite chernozem (unit 11 – IHS 3a and 3b) is dated to 73.70 ± 4.67 ka (BT 756), and corresponds to the end of MIS 5a. The upper sub-unit 11, IHS 3b, can be correlated with GIS 20. Taking into account this dating, the lower horizon of unit 11, IHS 3a, corresponds most likely to GIS 21. Finally the succession formed by units 10 and 9 represent the last pedosedimentary cycle of subsequence I, with unit 9 showing a weak humic pedogenesis (IHS 4). Considering the age of BT 757 (71.27 ± 4.86 ka) obtained for the upper part of unit 9, this part of the section (IHS 4) could represent the last short interstadial, GIS 19, of the Early Glacial, representing the boundary between MIS 5a and MIS 4 (Martinson, et al., 1987) (Fig. 7).

3. Interpretation

3.1. STADIAL STORMS AS dust Depositors

Marker silts (MS) are generally finer grained than normal loess but no significant differences are found in the petrological content or even in the magnetic fabric (Hradilova, 1994, Hradilova and Stastny, 1994). The new results presented in the previous section on the classical DV sequence do not differ from previous descriptions on this point. The source of the dust in the MS layers is, therefore, even more intriguing.

This source could not have been lying close to the location of this soil record, as the surface in the vicinity was covered by black, mostly decalcified and degraded chernozems under grass cover, while the local rivers carried decalcified detritus from the surrounding highlands (Kukla, 1977, Rousseau, et al., 1998). These grey-whitish MS silts must, therewith, be due to long-distance wind transport because of the sharp boundaries between these silts and the adjacent layers. Since the granular composition of the MS layers is much finer than that of loess — with a grain fraction in the range of 0.05 to 0.125 mm, a fraction that can still be moved by local winds — the latter would have caused a much more gradual mixing between the MS and loess layers. This interpretation seems to apply to the eolian silts observed in the DV stratigraphy as well. Furthermore, the chemical, magnetic, and basic mineralogical composition of the MS silts is similar to that of the overlying loess.

The modeling experiments of (Sima, et al., 2009) on dust emission for stadial conditions in western Europe show that ground surface conditions are most favorable in spring for both the emission and transport of fine-grained material. These favorable conditions arise after harsher winter conditions and before the start of the development of the vegetation, later in the season; the optimal time for dust emission and transport is slightly shifted towards early summer during Heinrich events.

Considering the new OSL dates (Fuchs, et al., 2012) and the proposed correlation with Greenland ice-core records, both MS and ES events in the DV sequence can be linked to several cold events identified in the North Atlantic Ocean (McManus, et al., 1994). These cold events have also been associated with drastic vegetation changes in the La Grande Pile pollen sequence (Kukla, et al., 1997).

The pollen record in the peat bog at La Grande Pile is located on the southern edge of the Vosges Mountain. This record indicates that, at the time of MS and ES deposition at DV, the vegetation was particularly poor (80 % of non-arboreal pollen), with steppe conditions over an open landscape (Woillard, 1978). These intervals are named the Ognon stadial II, Melisey II, St. Germain I 5b, Montaigu, Melisey I and Woillard events (Kukla, et al., 1997, Rousseau, et al.,

2006, Woillard, 1978). Scarce vegetation at European mid-latitudes, the contrasted seasonal regime of rivers, and the lowering of the sea level are all favorable conditions for the mobilization of fine material.

Marine records provide complementary information about the continental glaciers but also about ice-sheet behavior. Marine core V29-191 (McManus, et al., 1994) indicates that during the continental stadials Melisey I and II, and at the MIS 5/4 boundary, the North Atlantic experienced iceberg discharges named cold events C24 and 21 (McManus, et al., 1994), relabeled GS24-NAC24 and GS21-NAC21 by (Rousseau, et al., 2006). Such cold events indicate the occurrence of continental ice sheets able to veal icebergs that carried ice-rafted material through the ocean (Kukla, et al., 1997). These ice sheets are obviously large enough to contribute to the production of fine material, available in their front moraines. Core V29-191 also yielded evidence that during the cold events NAC24, 21 and 20, surface waters contained high percentages of Neogloboquadrina pachyderma sinistral (Fig. 7). Such an increase in cold-temperature planktonic foraminifera suggests an advance of the polar front in this area (McManus, et al., 1994), constraining therefore the path of the depressions over Europe.

While the size of these stadial ice sheets was large enough to generate icebergs, Kutzbach et al. (1993) concluded, though, that they did not produce a substantial climatological deviation of the polar jet stream, as reconstructed at the last glacial maximum (Kutzbach, et al., 1993, Manabe and Broccoli, 1985). Therefore, one or more other mechanisms must be considered to induce strong winds over Europe that could help build the observed units of dust and silt at the DV site.

MS units occur in Central European loess sequences in a precise geomorphological context, namely slope deposition. Their westernmost occurrence is in the Rhine River valley in Germany (Seelos and Sirocko, 2007) and in Alsace, where Rousseau and co-workers recognized the original Marker II (Rousseau, et al., 1998, 1998). In this area, the MS units are well preserved and they follow the stratigraphic succession described by Kukla and Lozek (1961) for Czech and Slovakian deposits. In other sites in Northern France, however, eolian deposits documented

in basal pedocomplexes correspond to a loess deposit (Antoine, et al., 1999), while in Ukraine, eolian silts at Vyazivok Tyasmyn and Pryluky have also been observed during MIS 5, and interpreted as strictly coeval with marker silts (Rousseau, et al., 2001).

In the context of peat deposits, Seret et al. (1990) noticed the occurrence of eolian elements in the Grande Pile stratigraphy. They showed that wind-blown sediments are mostly observed during the Melisey I and II stadials. We propose therewith that marker silts are distributed throughout the western part of the Eurasian continent, from the Rhine valley to the Dnieper plain in western Ukraine. ES layers could have been similarly distributed as well, which seems remarkable as this area shows a particular geomorphological context with the main relief, the Alps, oriented W-E.

Dust storms of continental extent seem, therefore, to be the most appropriate candidate for a satisfactory explanation of the deposition of the marker and eolian silts during MIS 5. This interpretation of the European loess series appears to be at present the most plausible one, with a succession of major dust events during Greenland stadials, especially those that record, across the European corridor at 51° N, the abrupt climate changes of MIS 3 and 2 (Rousseau, et al., 2007) (Fig. 2).

3.2. Dust storms and climate

Numerous reports present major dust events worldwide. However, these events are rather rare in Europe, despite the transport of African dust towards Western Europe across the Mediterranean (Dalmeida, 1986). Kukla (1975) reported that on 5 April 1960, a storm deposited three centimeters of dust over parts of Romania, and that this dust was carried from the Kalmyk steppe in Central Asia, i.e. a distance of over 2 000 kilometers. Recently, several dust storms were reported in China in April 1990 (Zhang, et al., 1991), while a particularly strong one occurred in May 1993 (Derbyshire, et al., 1998, Shao and Dong, 2006, Wang, et al., 2004).

The 2001 dust event in China is considered as the strongest one ever recorded, in its intensity as well as in the extent of its coverage: $2.5 \cdot 10^8$ metric tons of particles were released into the atmosphere. This event lasted for 10 days, from the dust emission into the atmosphere until the first deposition on the other side of the Pacific, on the West Coast of North America (Gong, et al., 2003, Simpson, et al., 2003). The more recent Australian (Choobari, et al., 2012) and United States dust events — in 2009 and in 2010, respectively — were also large-amplitude phenomena that could serve as plausible analogs for similar events during interglacial dust intervals.

Several climatic elements characterize these modern dust storms. First, the dust emission is linked to total lack of or, at least, depletion of vegetation cover, and to a land surface condition that reduces precipitation, at least on a regional scale. Furthermore, the long-range dust transport implies, following Pye (1987):

a) strong heating of the ground, which leads to the formation of a deep mixed layer;

b) an upper-level momentum source, which is linked to the occurrence of a cold front that produces ascending trajectories and a large-scale convergence;

c) an enhanced horizontal pressure gradient, associated with a particular circulation pattern.

The characteristics of inferred past dust events during the above-mentioned stadials fit this characterization of weather conditions during dust storms relatively well. Substantial uncertainties in the identification of these conditions remain, however, due to: (i) the exact timing of the paleo-dust events; (ii) the origin of the material; (iii) the climatic scenario under which the dust deposits occurred; and (iv) the most likely mechanism responsible for the dust events. We now consider and attempt to remove these uncertainties, one by one.

3.2.1. Exact timing of our paleo-dust events

The overall position of the silt events in the stratigraphy of the bottom of the last climate cycle is given in Fig. 6. The error bars related to the dating method prevent, however, the

identification of the exact timing of these continental dust events. Still, the new OSL dates support the correlations with the cold events observed in the marine cores and with the vegetation changes in continental records. From these correlations, one can estimate that silt events last for about 2 ka.

3.2.2. Origin of the material and duration of the dust events

Dust peaks preserved in the Greenland GRIP record also correspond to the dust units observed in the continental record (Fig. 7). This agreement suggests that both types of dust records arise due to the same general atmospheric circulation pattern, even without having to assume the same origin for the dust deposited in the two locations. Indeed, the duration of Greenland stadials is of 1885 ± 835 yrs, on the average, according to the NGRIP 2004 timescale (Andersen, et al., 2004). Therefore the dust events identified in the DV records last for about 2000 years.

This duration can be interpreted in two ways. The first interpretation is to assume that each silt unit corresponds to a single event, which lasted for the whole duration of the unit's deposition; such an interpretation is, however, highly unrealistic. The second interpretation is that each silt unit corresponds to a succession of short events. Each such event would have lasted at most several days, as do the present-day dust storms, it would have occurred during a particular season of the year, and it would have been preserved in the stratigraphy under favorable conditions. The dust record obtained by the Eifel Laminated Sediment Archive (ELSA) project in the cores retrieved from Eifel maar lakes supports such an interpretation. These cores cover the last climate cycle and they also record dust events, interpreted as loess, which are matching several cold events observed in the North Atlantic's NAC26 to NAC18 stadials; the last three of these are of minor magnitude compared to the older ones (Seelos and Sirocko, 2007).

3.2.3. Climatic scenarios for ES and MS units

458 We showed so far that the soil complexes of the DV loess sequence recorded the main
459 climate events of MIS 5 and 4, in agreement with Greenland ice cores and other climate records
460 of the last glacial cycle, as indicated in Figs. 6 and 7. In particular, the well-dated $\delta^{18}O$ record
461 from speleothems located along the northern rime of the Alps yield interesting results, indicated
462 by the curve labeled NALPS in Fig. 7. First of all, these speleothems record the climate changes
463 described in Greenland ice cores, especially the warm D/O interstadials. Hiatuses and light $\delta^{18}O$
464 values correspond to the Greenland stadials, as well as to the cold events (C) described in the
465 North Atlantic by McManus et al. (1994) (Fig. 7).

466 The oxygen isotope composition of the speleothems is representative of the regional
467 precipitation; in the Northern Alps, the precipitation originates mainly from the North Atlantic
468 and from Central European land areas (Sodemann and Zubler, 2010). A look at the NALPS
469 record during MIS 5 reveals that the ES events, as well as the interstadials, show a moisture
470 transport that must originate from oceanic areas to the west, like in the modern atmospheric
471 flow pattern of dominant westerlies. The hiatuses in the NALPS $\delta^{18}O$ record, however, are
472 correlated with the occurrence of the MS units and indicate a lack of moisture supply from the
473 west, leading us to surmise that another circulation pattern prevailed during these time intervals.

474 Annual precipitation estimates reconstructed from the Grande Pile pollen record
475 indicate low precipitation — of about 500 mm vs. the modern 1 080 mm — during the time
476 interval that corresponds to the deposition of the first Marker (Rousseau, et al., 2006). Such a
477 low precipitation amount implies particularly dry conditions, which are highly favorable for
478 dust emission. By extension, we propose here that the marker silts deposited during MIS 5 are
479 due to an atmospheric circulation pattern that differed from the one prevailing during the rest of
480 the record. In other words, these dust events testify to atmospheric conditions that are unlike
481 those recorded during the rest of MIS 5, but also unlike those associated with the loess
482 deposition during the glacial interval of MIS 4, 3 and 2 over Europe (Sima, et al., 2009).

483

484 3.2.4. Blocking structure and polar air outbreaks over Europe.

To seek an explanation of the dust events that gave rise to the marker silts, we need to consider mechanisms of meridional air-mass dynamics and energy exchanges. At present, the mid-latitudes of the Northern Hemisphere (NH) are dominated by westerly zonal flow, which is stronger in winter than in summer (Lorenz, 1967, Peixoto and Oort, 1992). Even now, the dominant westerlies in the NH have a stronger wavy component than in the Southern Hemisphere, due to the former's greater continentality; the NH continents induce quasi-permanent ridges and troughs into the westerly flow due to both topographic and thermal effects (Charney and Eliassen, 1949, Hoskins and Pearce, 1983). Marengo and Rogers (2001) recently made some of the same points in a paleoclimatic context.

The meridional component of the NH flow is occasionally strengthened during blocking events (Charney and Devore, 1979, Namias, 1950, Rossby, 1939). The frequency, duration and predictability of blocking events have been an active area of research in dynamic meteorology for the last few decades (Ghil and Childress, 1987, Ghil and Robertson, 2002). The idea that the frequency and duration of these events might change as a cause, manifestation or consequence of climate change goes back at least to Rex (1950) and has been further examined in Chapter 6 of Ghil and Childress (1987) and by Corti et al. (1999), among others. Slonosky et al. (2000) have documented such changes in European climate over the last two centuries.

The presence of a blocking ridge favors polar air outbreaks. These air masses originate in high latitudes; they are organized into mobile high-pressure lenses of nearly circular shape and of relatively large scale, being 2000–3000 km in diameter, and they migrate into the mid-latitudes by cold-air advection. Their migration is rapid and their path is controlled by the continental topography, the thickness of the air mass, and the precise location of the blocking ridge (Fig. 8). These outbreaks occur when the pole-to-equator temperature gradient is high (Namias, 1950), which is the case during the cold seasons, i.e., in NH fall to spring.

D'Andrea et al. (1998) carried out a comparison of climate simulations with 15 general circulation models (GCMs), and noticed the prevalence of blocking events over the Euro-Atlantic sector in late winter and spring. These are precisely the seasons that Sima et al. (2009)

512 recognized as the most favorable for dust emission under stadial conditions. Polar air outbreaks
513 are thus a likely mechanism for the dust events we wish to explain herein, since they are
514 associated with rapid low-level airstreams.

515 An amplification of this mechanism is to be expected during stadial intervals, when Europe
516 experienced colder conditions than at present. During such a colder climate, mid-latitude
517 disturbances were more violent as a result of stronger temperature contrasts between polar and
518 temperate air masses. Climate variations calculated for stadial conditions across the 51°N
519 parallel (Sima, et al., 2009) show high gradients in spring, which yield a frontal condition of
520 cold air masses moving over a heated surface. Such conditions, in turn, favor strong vertical
521 motion over open landscapes with reduced vegetation. All these elements enhance dust
522 emission and subsequent dust storms of continental magnitude in late winter and spring, while
523 they are much reduced or totally inexistent in summer.

524 In Western and Central Europe, the main relief is basically oriented NE–SW in Scandinavia
525 and West–East for the Alps further south. This distribution of elevated areas (Rex, 1950) was
526 probably enhanced by the occurrence of larger mountain-massif ice caps during the stadials, an
527 enhancement that was likely to strengthen air-mass exchanges with respect to present-day
528 conditions, and thus contribute to the deposition of the marker silts. The polar-air outbreaks
529 were channeled into a West–East corridor, between Scandinavia and the Alps, that corresponds,
530 in fact, to the western part of the loess belt (Fig. 2).

531 A similar topographic pattern was responsible for the May 1993 dust storm in China
532 (Derbyshire, et al., 1998, Shao and Dong, 2006, Wang, et al., 2004), when an intense frontal
533 system over Siberia generated an unusually cold and massive airflow in the Hexi corridor of
534 northern China. Combined with the strong thermal gradient between a warming Tibetan Plateau
535 to the south and the cold Siberian plain (Shao and Dong, 2006), the channeling of this unusual
536 airflow by the topographic effect of the Altai and Tianshan Mountains led to the so-called “dark
537 storm” (Shao and Dong, 2006, Wang, et al., 2004) that affected several provinces, over a total
538 area of the size of France and Spain combined. The paleoclimatic role of this corridor in the

accumulation of the loess deposits of Gansu province was discussed by Derbyshire et al. (1998), among others. Similarly, the dust events over China in 2001, Australia in 2009 and the United States in 2011 were all related to cold-front dynamics.

On the contrary, east of the Central-European corridor whose southern border are the Alps, beyond the Carpathians, no noticeable topography is present, until the North-South–oriented Urals. Over this East-European Plain, the absence of topographic constraints implies a serious drop in the wind velocity. As a consequence, while markers still occur in the western Ukraine (see Fig. 2), they appear to be totally absent further east, until high, West-East–oriented reliefs are present again in Tajikistan.

The climatic scenario described in the preceding paragraphs is a plausible state of affairs for the lower part of the last climatic cycle, before full glacial conditions were reached. The synchronicity of the first main dust events in the Greenland ice cores and in the pedocomplexes of the European loess sequences cannot be purely a matter of chance. On the contrary, the arguments above suggest that these short intervals correspond to specific atmospheric conditions over both high and mid-latitudes in the Euro-Atlantic sector, and generally poor vegetation conditions in European mid-latitudes. Given the topographic pattern of western and central Europe, these atmospheric and vegetation conditions provide a plausible explanation of the phenomena that we set out to clarify here.

The occurrence of marker silts in Central Europe while loess was deposited in Western Europe is in agreement with the general scenario proposed by Pye and Zhou (1989) and by Pye (1995). In their scenario of eolian deposits, long-range transport of dust is favored when dust is lifted ahead of cold fronts and incorporated into the upper-level westerlies, while dry fallout from low-level dust clouds forms loess deposits in greater proximity to the dust sources. Marine core V29-191 indicates that the polar front advanced at the time of the sedimentation of the MS units (McManus, et al., 1994); Fig. 7). Our hypothesis of the enhancement of blocking activity and polar-air outbreaks during this sedimentation provides the missing origin of regional-scale wind patterns necessary for long-range transport and formation of distal deposits.

4. Conclusion

Large-scale continental dust storms are common at present in eastern Asia, Africa and Australia. They represent extreme events (Ghil, et al., 2011) that cause major hazards for the population, the livestock and the vegetation of the large regions affected. Reports on the May 1993 dust storm in northwestern China documented huge, wall-like clouds of dust moving rapidly in a direction that lead from a high-pressure cell over Siberia to a low-pressure one over southern China. Complete darkness at noon occurred, trees were uprooted or broken, many animals and several people were killed, and a significant layer of dust covered crops. Another dust event, even stronger than the 1993 one, was recorded in April 2001; the latter event led to the export of large amounts of material from the Gobi Desert towards North America and, in some places, combined with locally generated urban pollution there.

Except for rains conveying dust from the Sahara, most of Europe does not experience at present continental dust storms. During the previous interglacial and early glacial period, however, striking eolian-silt deposits have been found in loess sequences: these deposits correspond to fine-grained material that has been interpreted as the fingerprint of large-scale dust events.

The penultimate interglacial and early glacial, equivalent to marine stage MIS 5, experienced major dust events that have left their imprint on European terrestrial records. These events are clearly visible in loess sequences by their whitish color (L* of about 50%), overlying and underlying dark chernozem paleosols of MIS-5 age. They are mostly recorded in Central Europe and their western limit appears to be the Rhine River valley.

We described here the base of the Dolni Vestonice (Czech Republic) loess sequence (Fig. 3 and 5 here) as the reference for these stratigraphic horizons. Such units were formed during

intervals characterized by sparse vegetation — as identified by high $\delta^{13}C$ values and low magnetic susceptibility — and they show finer grain size values, lower percentages in fine sand and higher ones in clay content than the overlying pleniglacial loess deposits.

G. Kukla and associates described some of these dust horizons as "markers" in the 1960s and early 1970s (Kukla and Lozek, 1961, Kukla and Koci, 1972, Kukla, 1975, 1977, Kukla, 1961); see Fig. 4 here); they are dated at about 111–109 ka and 93–2 ka, a last one being slightly visible at about 75–73 ka. Other dust horizons have been described as eolian silts (ES) and correspond to the loess material of Kukla's cycles. The ES units are observed in the same sequence and are dated at about 106–105 ka, 88–86 ka, and 78.5–77 ka.

All these eolian horizons correspond to short events of about 2 ka in duration on the average; they are synchronous with advances of the polar front over the North Atlantic, as recorded in marine cores as cold (C) events (Figs. 5–7 here). They also correlate with abrupt changes observed in European vegetation. The comparison with the $\delta^{18}O$ record from Northern Alps speleothems shows that, while ES appear to be coeval with moisture supply from the North Atlantic, the marker silts do not show such a relationship. This decoupling between the two modes of dust deposition during MIS 5 differs from the pleniglacial situation, in which loess sedimentation in Europe tracks the Greenland dust record, while it is consistent with westerly transport. We conclude that the occurrence of these dust events in the MIS 5 stratigraphy corresponds to a climatic mechanism that links polar-air outbreaks to blocking action associated with atmospheric circulation patterns that favor meridional flow.

Acknowledgements

This study is supported by the French Agence Nationale pour la Recherche (ANR) through the ACTES project ANR-08-BLAN-0227/CSD-6 at the Ecole Normale Supérieure, and through grant DE-SC0006694 from the U.S. Department of Energy and grant DMS-0934426 from the U.S. National Science Foundation at UCLA. This is LDEO contribution 2012-yyy.

620

621 References

622

623 An, Z. S., Kukla, G., Porter, S. C., Xiao, J. L., 1991. Magnetic susceptibility evidence of
624 monsoon variation on the loess plateau of Central China during the last 130,000 years.
625 Quaternary Res. 36, 29-36.
626 Andersen, K. K., Azuma, N., Barnola, J. M., Bigler, M., Biscaye, P., Caillon, N., Chappellaz, J.,
627 Clausen, H. B., DahlJensen, D., Fischer, H., Fluckiger, J., Fritzsche, D., Fujii, Y., Goto-
628 Azuma, K., Gronvold, K., Gundestrup, N. S., Hansson, M., Huber, C., Hvidberg, C. S.,
629 Johnsen, S. J., Jonsell, U., Jouzel, J., Kipfstuhl, S., Landais, A., Leuenberger, M.,
630 Lorrain, R., Masson-Delmotte, V., Miller, H., Motoyama, H., Narita, H., Popp, T.,
631 Rasmussen, S. O., Raynaud, D., Rothlisberger, R., Ruth, U., Samyn, D., Schwander, J.,
632 Shoji, H., Siggard-Andersen, M. L., Steffensen, J. P., Stocker, T., Sveinbjornsdottir, A.
633 E., Svensson, A., Takata, M., Tison, J. L., Thorsteinsson, T., Watanabe, O., Wilhelms,
634 F., White, J. W. C., Project, N. G. I. C., 2004. High-resolution record of Northern
635 Hemisphere climate extending into the last interglacial period, Nature 431, 147-151.
636 Antoine, P., Rousseau, D. D., Lautridou, J. P., Hatté, C., 1999. Last interglacial-glacial climatic
637 cycle in loess-paleosol successions of north-western France, Boreas 28, 551-563.
638 Antoine, P., Rousseau, D. D., Moine, O., Kunesch, S., Hatte, C., Lang, A., Tissoux, H., Zöller,
639 L., 2009. Rapid and cyclic aeolian deposition during the Last Glacial in European loess:
640 a high-resolution record from Nussloch, Germany, Quaternary Sci. Rev. 28, 2955-2973.

641

642

643 Antoine, P., Rousseau, D.D., Degeai, J.P., Moine, O., Lagroix, F., Kreutzer, S., Fuchs, M.,
644 Hatté, C., Gauthier, C., Svoboda, J., Lisa, L. High-resolution record of the
645 environmental response to climatic variations during the last interglacial-glacial cycle in

Central Europe: the loess-palaeosol sequence of Dolní Věstonice (Czech Republic). Quaternary Sci. Rev. (soumis)

Biscaye, P. E., Grousset, F. E., Revel, M., Van der Gaast, S., Zielinski, G. A., Vaars, A., Kukla, G., 1997. Asian provenance of glacial dust (Stage 2) in the GISP2 ice core, summit, Greenland, J. Geophys. Res. 102, 26,765-726,781.

Boch, R., Cheng, H., Spotl, C., Edwards, R. L., Wang, X., Hauselmann, P., 2011. NALPS: a precisely dated European climate record 120-60 ka, Clim. Past 7, 1247-1259.

Bond, G., Heinrich, H., Broecker, W., Labeyrie, L., McManus, J., Andrews, J., Huon, S., Jantschik, R., Clasen, S., Simet, C., Tedesco, K., Klas, M., Bonani, G., Ivy, S., 1992. Evidence for massive discharges of icebergs into the North Atlantic Ocean during the last glacial period., Nature 360, 245-249.

Bond, G. C., Lotti, R., 1995. Iceberg discharges into the North Atlantic on millennial time scales during the last glaciation., Science 267, 1005-1010.

Bory, A. J. M., Biscaye, P. E., Svensson, A., Grousset, F. E., 2002. Seasonal variability in the origin of recent atmospheric mineral dust at NorthGRIP, Greenland, Earth Planet. Sc. Lett. 196, 123-134.

Chappellaz, J., Brook, E., Blunier, T., Malaizé, B., 1997. CH_4 and $\delta^{18}O$ of O_2 records from Antarctic and Greenland ice: A clue for stratigraphic disturbance in the bottom part of the Greenland Ice Core Project and the Greenland Ice Sheet Project 2 ice cores, J. Geophys. Res. 102, 26,547-526,557.

Charney, J. G., Eliassen, A., 1949. A numerical method for predicting the perturbations of the middle latitude westerlies, Tellus 1, 38-54.

Charney, J. G., Devore, J. G., 1979. Multiple flow equilibria in the atmosphere and blocking, J. Atmos. Sci. 36, 1205-1216.

Choobari, O. A., Zawar-Reza, P., Sturman, A., 2012. Atmospheric forcing of the three-dimensional distribution of dust particles over Australia: A case study, J. Geophys. Res. 117, DOI: 10.1029/2012JD017748.

673 Corti, S., Molteni, F., Palmer, T. N., 1999. Signature of recent climate change in frequencies of
674 natural atmospheric circulation regimes, Nature 398, 799-802.
675 D'Andrea, F., Tibaldi, S., Blackburn, M., Boer, G., Deque, M., Dix, M. R., Dugas, B., Ferranti,
676 L., Iwasaki, T., Kitoh, A., Pope, V., Randall, D., Roeckner, E., Straus, D., Stern, W.,
677 Van den Dool, H., Williamson, D., 1998. Northern Hemisphere atmospheric blocking
678 as simulated by 15 atmospheric general circulation models in the period 1979-1988,
679 Clim. Dynam. 14, 385-407.
680 Dalmeida, G. A., 1986. A model for Saharan dust transport, J. Clim. Applied Meteor. 25, 903-
681 916.
682 Dansgaard, W., Clausen, H. B., Gundestrup, N., Hammer, C. U. J., Johnsen, S. F.,
683 Kristinsdottir, P. M., Reeh, N., 1982. A new Greenland deep ice core., Science 218,
684 1273-1277.
685 Dansgaard, W., Oeschger, H., 1989. Past environmental long-term records from the Arctic, in:
686 H. Oeschger, C.C. Langway, (Eds), The Environmental Record in Glaciers and Ice
687 Sheets, John Wiley & Sons, Chichester, pp. 287-318.
688 Dansgaard, W., Johnsen, S. J., Clausen, H. B., Dahi-Jensen, D., Gundestrup, N. S., Hammer, C.
689 U., Hvidberg, C. S., Steffensen, J. P., Sveinbjörnsdottir, A. E., Jouzel, J., Bond, G.,
690 1993. Evidence for general instability of past climate from a 250-kyr ice-core record.,
691 Nature 364, 218-220.
692 Dansggard, W., Clausen, H. B., Gundestrup, N., Johnsen, S. F., Rygner, C., 1985. Dating and
693 climatic interpretation of two deep Greenland ice cores, in: C.C. Langway, H.
694 Oeschger, W. Dansgaard, (Eds), Greenland Ice Core: Geophysics, Geochemistry, and
695 the Environment 33, Geophysical Monograph, pp. 71-76.
696 Debret, M., Sebag, D., Desmet, M., Balsam, W., Copard, Y., Mourier, B., Susperrigui, A. S.,
697 Arnaud, F., Bentaleb, I., Chapron, E., Lallier-Verges, E., Winiarski, T., 2011.
698 Spectrocolorimetric interpretation of sedimentary dynamics: The new "Q7/4 diagram",
699 Earth-Rev. Rev. 109, 1-19.

Demek, J., Kukla, J., 1969. Periglazialzone, löss und paläolithikum der Tschechoslowakei, Czechoslovak Academy of Sciences, Institute of Geography, Brno, Brno.

Derbyshire, E., Meng, X. M., Kemp, R. A., 1998. Provenance, transport and characteristics of modern aeolian dust in western Gansu Province, China, and interpretation of the Quaternary loess record, J. Arid Environ. 39, 497-516.

Ding, Z. L., Rutter, N., Han, J. T., Liu, T. S., 1992. A coupled environmental system formed at about 2.5 Ma in East Asia., Palaeogeogr. Palaeocl. 94, 223-242.

Ding, Z. L., Ren, J. Z., Yang, S. L., Liu, T. S., 1999. Climate instability during the penultimate glaciation: Evidence from two high-resolution loess records, China, J. Geophys. Res. 104, 20123-20132.

Ding, Z. L., Ranov, V., Yang, S. L., Finaev, A., Han, J. M., Wang, G. A., 2002. The loess record in southern Tajikistan and correlation with Chinese loess, Earth Planet. Sc. Lett. 200, 387-400.

Fischer, H., Siggaard-Andersen, M. L., Ruth, U., Rothlisberger, R., Wolff, E., 2007. Glacial/interglacial changes in mineral dust and sea-salt records in polar ice cores: Sources, transport, and deposition, Rev. Geophys. 45, DOI: 10.1029/2005RG000192.

Forster, T., Heller, F., 1994. Loess deposits from the Tajik depression (Central Asia): Magnetic properties and paleoclimate, Earth Planet. Sc. Lett. 128, 501-512.

Fuchs, M., Kreutzer, S., Rousseau, D. D., Antoine, P., Hatté, C., Lagroix, F., Moine, O., Gauthier, C., Svoboda, J., Lisa, L., 2012. The loess sequence of Dolni Vestonice, Czech Republic: A new OSL-based chronology of the Last Climatic Cycle, Boreas (in press).

Ghil, M., Childress, S., 1987. Topics in Geophysical Fluid Dynamics: Atmospheric Dynamics, Dynamo Theory and Climate Dynamics, Springer-Verlag, New-York.

Ghil, M., Robertson, A. W., 2002. "Waves"' vs. "particles"" in the atmosphere's phase space: A pathway to long-range forecasting?, P. Natl. Acad. Sci. USA 99, 2493-2500.

Ghil, M., Yiou, P., Hallegatte, S., Malamud, B. D., Naveau, P., Soloviev, A., Friederichs, P., Keilis-Borok, V., Kondrashov, D., Kossobokov, V., Mestre, O., Nicolis, C., Rust, H.

W., Shebalin, P., Vrac, M., Witt, A., Zaliapin, I., 2011. Extreme events: dynamics, statistics and prediction, Nonlinear Proc. Geoph. 18, 295-350.

Gong, S. L., Zhang, X. Y., Zhao, T. L., McKendry, I. G., Jaffe, D. A., Lu, N. M., 2003. Characterization of soil dust aerosol in China and its transport and distribution during 2001 ACE-Asia: 2. Model simulation and validation, J. Geophys. Res. 108, D9, DOI: 10.1029/2002JD002633.

GRIP members, 1993. Climate instability during the last interglacial period recorded in the GRIP ice core, Nature 364, 203-207.

Gu, Z., Liu, R., Liu, Y., 1991. Response of the stable isotopic composition of loess-paleosol carbonate to paleoenvironmental changes., in: L. T, (Ed), Loess, environment and global change, Science Press, Beijing, pp. 82-92.

Guo, Z., Liu, T., Guiot, J., Wu, N., Lü, H., Han, J., Liu, J., Gu, Z., 1996. High frequency pulses of East Asian monsoon climate in the last two glaciations: link with the North Atlantic., Clim. Dynam. 12, 701-709.

Guo, Z. T., Ruddiman, W. F., Hao, Q. Z., Wu, H. B., Qiao, Y. S., Zhu, R. X., Peng, S. Z., Wei, J. J., Yuan, B. Y., Liu, T. S., 2002. Onset of Asian desertification by 22 Myr ago inferred from loess deposits in China, Nature 416, 159-163.

Hammer, C. U., Clausen, H. B., Dansgaard, D., Neftel, A., Kristinsdottir, P., Johnson, E., 1985. Continuous impurity analysis along the Dye 3 deep core, in: C.C. Langway, H. Oeschger, W. Dansgaard, (Eds), Greenland ice core : Geophysics, Geochemistry and the Environment 33, Geophysical Monograph, pp. 90-94.

Hatté, C., Antoine, P., Fontugne, M., Rousseau, D. D., Tisnérat-Laborde, N., Zöller, L., 1999. New chronology and organic matter $\delta^{13}C$ paleoclimatic significance of Nussloch loess sequence (Rhine Valley, Germany), Quatern. Int. 62, 85-91.

Heinrich, H., 1988. Origin and consequences of cyclic ice rafting in the Northeast Atlantic Ocean during the past 130,000 years, Quaternary Res. 29, 142-152.

753 Heller, F., Liu, T. S., 1982. Magnetostratigraphical dating of loess deposits in China., Nature
754 300, 1169-1172.
755 Heller, F., Liu, X., Liu, T., Xu, T., 1991. Magnetic susceptibility of loess in China, Earth Planet.
756 Sc. Lett. 103, 301-310.
757 Hesse, P. P., McTainsh, G. H., 2003. Australian dust deposits: modern processes and the
758 Quaternary record, Quaternary Sci. Rev. 22, 2007-2035.
759 Hoskins, B. J., Pearce, R. P., 1983. Large-Scale Dynamic Processes in the Atmosphere,
760 Academic Press, London/New York.
761 Hradilova, J., 1994. New micromorphological knowledge of the last Pleistocene glacial cycle in
762 the loess profile at Praha-Sedlec, J. Czech Geol. Soc. 39/4, 319-329.
763 Hradilova, J., Stastny, M., 1994. Changes in the clay fraction mineral composition in a loess
764 profile of the last interglacial and early glacial in Praha-Sedlec, Acta Univ. Carol. Geol.
765 38, 229-238.
766 Johnsen, S. J., Dahl-Jensen, D., Gundestrup, N., Steffensen, J. P., Clausen, H. B., Miller, H.,
767 Masson-Delmotte, V., Sveinbjörnsdottir, A. E., White, J., 2001. Oxygen isotope and
768 palaeotemperature records from six Greenland ice-core stations: Camp Century, Dye-3,
769 GRIP, GISP2, Renland and NorthGRIP, J. Quaternary Sci. 16, 299-307.
770 Kukla, G., Lozek, V., 1961. Loess and related deposits. In Survey of Czechoslovak Quaternary.
771 Czwartozed Europy Srodkowej i Wschodniej. INQUA 6th Int. Congr., Inst. Geol.
772 Prace, Warszawa, 34, 11-28.
773 Kukla, G., Koci, A., 1972. End of the last interglacial in the loess record, Quaternary Res. 2,
774 374-383.
775 Kukla, G., 1975. Loess stratigraphy of central Europe., in: K.W. Butzer, G.L. Isaac, (Eds),
776 After the Australopithecines, Mouton, The Hague, pp. 99-188.
777 Kukla, G., 1977. Pleistocene land-sea correlations. 1. Europe., Earth-Rev. Rev. 13, 307-374.
778 Kukla, G., 1987. Loess stratigraphy in Central China., Quaternary Sci. Rev. 6, 191-219.

779 Kukla, G., Heller, F., Liu, X. M., Xu, T. C., Liu, T. S., An, Z. S., 1988. Pleistocene climates in
780 China dated by magnetic susceptibility., Geology 16, 811-814.
781 Kukla, G., McManus, J. F., Rousseau, D. D., Chuine, I., 1997. How long and how stable was
782 the last interglacial?, Quaternary Sci. Rev. 16, 605-612.
783 Kukla, G. J., 1961. Lithologische Leithorizonte der tschechoslowakischen Lössprofile, Véstnik
784 36, 369-372.
785 Kutzbach, J. E., Guetter, P. J., Behling, P. J., Selin, R., 1993. Simulated Climatic Changes:
786 Results of the COHMAP Climate-Model Experiments, in: J. Wright, H.E., J.E.
787 Kutzbach, T. Webb III, W.F. Ruddiman, F.A. Street-Perrott, P.J. Bartlein, (Eds), Global
788 Climates since the Last Glacial Maximum, University of Minnesota Press,
789 Minnneapolis, pp. 24-93.
790 Lang, A., Hatté, C., Rousseau, D. D., Antoine, P., Fontugne, M., Zöller, L., Hambach, U., 2003.
791 High-resolution chronologies for loess: comparing AMS^{14}C and optical dating results,
792 Quaternary Sci. Rev. 22, 953-959.
793 Liu, T. S., collaborators, 1985. Loess and the Environment, China Ocean Press, Beijing.
794 Lorenz, E. W., 1967. The Nature and Theory of the General Circulation of the Atmosphere,
795 Word Meteorological Organization, Geneva, Switzerland.
796 Lu, H., Wu, N., Nie, G., Wang, Y., 1991. Phytolith in loess and its bearing on paleovegetation,
797 The series of the XIII InQUA congress 112-123.
798 Manabe, S., Broccoli, A. J., 1985. The influence of continental ice sheets on the climate of an
799 ice-age, J. Geophys. Res. 90, 2167-2190.
800 Marengo, J. A., Rogers, J. C., 2001. Polar air outbreaks in the Americas: Assessments and
801 impacts during modern and past climates, in: V. Markgraf, (Ed), Interhemispheric
802 climate linkages, Academic Press, San Diego, pp. 31-51.
803 Martinson, D. G., Pisias, N. G., Hays, J. D., Imbrie, J., Moore, T. C., Shackleton, N. J., 1987.
804 Age dating and the orbital theory of the Ice ages: Development of a high-resolution 0 to
805 300,000-year chronostratigraphy, Quaternary Res. 27, 1-29.

McManus, J. F., Bond, G. C., Broecker, W. S., Johnsen, S., Labeyrie, L., Higgins, S., 1994. High-resolution climate records from the North Atlantic during the last interglacial., Nature 371, 326-329.

Namias, J., 1950. The index cycle and its role in the general circulation, J. Meteorol. 7, 130-139.

Pécsi, M., 1990. Loess is not just the accumulation of dust, Quatern. Int. 7/8, 1-21.

Peixoto, J. P., Oort, A. H., 1992. Physics of Climate, Springer Verlag, New-York/London.

Petit, J. R., Mounier, L., Jouzel, J., Korotkevivch, Y. S., Kotlyakov, V. I., Lorius, C., 1990. Palaeoclimatological and chronological implications of the Vostok core dust record., Nature 343, 56-58.

Porter, S. C., An, Z. S., 1995. Correlation between climate events in the North Atlantic and China during the last glaciation., Nature 375, 305-308.

Pye, K., 1987. Aeolian Dust and Dust Deposits., Academic Press.

Pye, K., Zhou, L. P., 1989. Late Pleistocene and Holocene aeolian dust deposition in North China and the Northwest Pacific Ocean., Palaeogeogr. Palaeocl. 73, 11-23.

Pye, K., 1995. The nature, origin and accumulation of loess, Quaternary Sci. Rev. 14, 653-657.

Rex, D. F., 1950. Blocking action in the middle troposphere and its effect upon regional climate. Part II: The climatology of blocking action, Tellus 2, 275-301.

Rossby, C. G., 1939. Relation between variations in the intensity of the zonal circulation of the atmosphere and the displacements of the semipermanent centers of action, J. Mar. Res. 2, 38-55.

Rousseau, D. D., Puisségur, J. J., 1990. A 350,000 years climatic record from the loess sequence of Achenheim, Alsace, France., Boreas 19, 203-216.

Rousseau, D. D., Puissegur, J. J., Lautridou, J. P., 1990. Biogeography of the Pleistocene Pleniglacial Malacofaunas in Europe - Stratigraphic and Climatic Implications, Palaeogeogr. Palaeocl. 80, 7-23.

832 Rousseau, D. D., 1991. Climatic transfer function from Quaternary molluscs in European loess
833 deposits., Quaternary Res. 36, 195-209.
834 Rousseau, D. D., Kukla, G., 1994. Late Pleistocene climate record in the Eustis loess section,
835 Nebraska, based on land snail assemblages and magnetic-susceptibility, Quaternary
836 Res. 42, 176-187.
837 Rousseau, D. D., Wu, N. Q., 1997. A new molluscan record of the monsoon variability over the
838 past 130 000 yr in the Luochuan loess sequence, China, Geology 25, 275-278.
839 Rousseau, D. D., Kukla, G., Zoller, L., Hradilova, J., 1998. Early Weichselian dust storm layer
840 at Achenheim in Alsace, France, Boreas 27, 200-207.
841 Rousseau, D. D., Zoller, L., Valet, J. P., 1998. Late Pleistocene climatic variations at
842 Achenheim, France, based on a magnetic susceptibility and TL chronology of loess,
843 Quaternary Res. 49, 255-263.
844 Rousseau, D. D., Gerasimenko, N., Matviischina, Z., Kukla, G., 2001. Late Pleistocene
845 environments of the Central Ukraine, Quaternary Res. 56, 349-356.
846 Rousseau, D. D., Antoine, P., Hatté, C., Lang, A., Zöller, L., Fontugne, M., Ben Othman, D.,
847 Luck, J. M., Moine, O., Labonne, M., Bentaleb, I., Jolly, D., 2002. Abrupt millennial
848 climatic changes from Nussloch (Germany) Upper Weichselian eolian records during
849 the Last Glaciation, Quaternary Sci. Rev. 21, 1577-1582.
850 Rousseau, D. D., Hatte, C., Guiot, J., Duzer, D., Schevin, P., Kukla, G., 2006. Reconstruction of
851 the Grande Pile Eemian using inverse modeling of biomes and δC^{13}, Quaternary Sci.
852 Rev. 25, 2806-2819.
853 Rousseau, D. D., Kukla, G., McManus, J., 2006. What is what in the ice and the ocean?,
854 Quaternary Sci. Rev. 25, 2025-2030.
855 Rousseau, D. D., Sima, A., Antoine, P., Hatte, C., Lang, A., Zöller, L., 2007. Link between
856 European and North Atlantic abrupt climate changes over the last glaciation, Geophys.
857 Res. Lett. 34, 22, DOI: 10.1029/2007GL031716.

858 Rousseau, D. D., Antoine, P., Gerasimenko, N., Sima, A., Fuchs, M., Hatte, C., Moine, O.,
859 Zoeller, L., 2011. North Atlantic abrupt climatic events of the last glacial period
860 recorded in Ukrainian loess deposits, Clim. Past 7, 221-234.
861 Ruth, U., Wagenbach, D., Steffensen, J. P., Bigler, M., 2003. Continuous record of
862 microparticle concentration and size distribution in the central Greenland NGRIP ice
863 core during the last glacial period, J. Geophys. Res. 108, D3, DOI:
864 10.1029/2002JD002376.
865 Seelos, K., Sirocko, F., 2007. Abrupt cooling events at the very end of the Last Interglacial, in:
866 F. Sirocko, M. Claussen, M.F. Sanchez Goni, T. Litt, (Eds), The Climate of Past
867 Interglacials 7, Elsevier, Amsterdam, pp. 207-229.
868 Seret, G., Dricot, E., Wansard, G., 1990. Evidence for an early glacial maximum in the French
869 Vosges during the last glacial cycle., Nature 346, 453-456.
870 Shackleton, N. J., An, Z., Dodonov, A. E., Gavin, J., Kukla, G. J., Ranov, V. A., Zhou, L. P.,
871 1995. Accumulation Rate of Loess in Tadjikistan and China: Relationship with Global
872 Ice Volume Cycles, Quaternary Proc. 4, 1-6.
873 Shao, Y., Dong, C. H., 2006. A review on East Asian dust storm climate, modelling and
874 monitoring, Global Planet. Change 52, 1-22.
875 Sima, A., Rousseau, D. D., Kageyama, M., Ramstein, G., Schulz, M., Balkanski, Y., Antoine,
876 P., Dulac, F., Hatte, C., 2009. Imprint of North-Atlantic abrupt climate changes on
877 western European loess deposits as viewed in a dust emission model, Quaternary Sci.
878 Rev. 28, 2851-2866.
879 Simpson, J. J., Hufford, G. L., Servranckx, R., Berg, J., Pieri, D., 2003. Airborne Asian dust:
880 case study of long-range transport and implications for the detection of volcanic ash,
881 Weather Forecast. 18, 121-141.
882 Slonosky, V. C., Jones, P. D., Davies, T. D., 2000. Variability of the surface atmospheric
883 circulation over Europe, 1774-1995, Int. J. Climatol. 20, 1875-1897.

884 Smiley, T. L., Bryson, R. A., King, J. E., Kukla, G. J., Smith, G. I., 1991. Quaternary
885 paleoclimates, in: R.B. Morrison, (Ed), Quaternary Nonglacial Geology: Conterminous
886 U.S. The Geology of North America K-2, The Geological Society of America, Boulder,
887 pp. 13-44.
888 Sodemann, H., Zubler, E., 2010. Seasonal and inter-annual variability of the moisture sources
889 for Alpine precipitation during 1995-2002, Int. J. Climatol. 30, 947-961.
890 Stuut, J. B., Zabel, M., Ratmeyer, V., Helmke, P., Schefuss, E., Lavik, G., Schneider, R., 2005.
891 Provenance of present-day eolian dust collected off NW Africa, J. Geophys. Res. 110,
892 D04202, doi:04210.01029/02004JD005161.
893 Svensson, A., Biscaye, P. E., Grousset, F. E., 2000. Characterization of late glacial continental
894 dust in the Greenland Ice Core Project ice core, J. Geophys. Res. 105, 4637-4656.
895 Tada, R., Irino, T., Koizumi, I., 1999. Land-ocean linkages over orbital and millennial
896 timescales recorded in late Quaternary sediments of the Japan Sea, Paleoceanography
897 14, 236-247.
898 Wang, X., Gong, Z., Zhang, J., Liu, L., 2004. Modern dust storms in China: An overview, J.
899 Arid Environ. 58, 559-574.
900 Wang, Y., Cheng, H., Edwards, R. L., Kong, X., Shao, X., Chen, S., Wu, J., Jiang, X., Wang,
901 X., An, Z., 2008. Millenial- and orbital-scale changes in the East Asian monsoon over
902 the past 224,000 years, Science 451, 1090-1093.
903 Wang, Y. J., Cheng, H., Edwards, R. L., An, Z. S., Wu, J. Y., Shen, C. C., Dorale, J. A., 2001.
904 A high-resolution absolute-dated late Pleistocene monsoon record from Hulu Cave,
905 China, Science 294. 2345-2348.
906 Woillard, G., 1978. Grande Pile peat bog : A continuous pollen record for the last 140,000
907 years, Quaternary Res. 9, 1-21.
908 Wu, N., Lu, H., Sun, X., Guo, Z., Liu, J., Han, J., 1995. Climatic factor transfer function from
909 opal phytolith and its application in paleoclimate reconstruction of China loess-paleosol

910 sequence, in: S. Wang, (Ed), Scientia Geologica Sinica, Science Press, Beijing, pp. 105-
911 114.
912 Zhang, G., Wang, X., Zhang, X., 1991. The synoptic dynamic condition and the features of
913 chemical elements of dustfall event in April 1990 in Beijing, in: T. Liu, (Ed), Loess,
914 Environment and Global Change, Science Press, Beijing, pp. 228-234.
915
916
917
918

919 Figure captions

920

921 Fig. 1. Greenland ice cores discussed in the text. a) Location of the GRIP and NGRIP
922 Greenland ice cores. b) Variation of the $\delta^{18}O$ (blue curve) and of the dust concentration (red
923 curve) during the last climate cycle in the GRIP ice core (Johnsen, et al., 2001) showing the
924 record of the abrupt warming named Dansgaard-Oeschger events associated with abrupt
925 decreases of the dust concentration.

926

927 Fig. 2. Location of major European loess sequences. The map also shows the distribution of the
928 loess deposits (in yellow) by thickness in Europe, as well as the extent of the continental ice
929 sheets (light blue) and the estimated lowering of the sea level (emerged areas in light gray) at
930 the last glacial maximum (P. Antoine, unpublished map, 2011).

931

932 Fig. 3. Stratigraphy of the last climate cycle at Dolni Vestonice (DV), Czech Republic adapted
933 from Antoine et al. (submitted). On the right is the chronostratigraphy, in terms of glaciation
934 cycles; in the middle is the pedostratigraphy, with the lithological succession of the soil
935 complexes PK = I, II, and III, according to Kukla (1975, 1977, Kukla, 1961); and on the left are
936 given visual snapshots of the sequence: (A) Penultimate climate cycle (Saalian loess) and the
937 interglacial Bt paleosol horizon; (B) PKIII and PKII soil complex succession; (C) Irregular top
938 of the upper chernozem of the PKII soil complex; (D) Mammoth bone in the Gravetian layer,
939 showing evidence of charcoal; and (E) sandy loess, showing wedges. Lithological log by P.
940 Antoine, in Fuchs et al. (2012), photos DDR.

941

942 Fig. 4. DV soil complexes. Comparison of the stratigraphy observed in 2009 (Fuchs, et al.,
943 2012) and the one described by B. Klima and G. Kukla in 1968, as published in (Demek and
944 Kukla, 1969).

945

946 Fig. 5. Continuous, quantitative characterization of the DV soil complexes. On the left are OSL
947 ages (mean ± error) and the DV pedostratigraphy. In the middle panel, from left to right: clay
948 content (%), black curve; low-frequency magnetic susceptibility (m^3kg^{-1}), red curve; total
949 carbonate content (%), blue curve; two spectrometric parameters — sediment brightness L*
950 (%), purple curve, and first-derivative spectrum FDS, red curve; and, finally, $\delta^{13}C$ from organic
951 matter, yellow curve. The FDS plotted here corresponds to the 555-nm band characteristic of
952 iron hydroxides such as goethite (cf. (Debret, et al., 2011)). On the right are the proposed
953 correlations with Greenland interstadials and marine isotope stratigraphy. Legend: Bt – Bt
954 paleosol horizon; IHS – isohumic soil; MS – marker silt; PS – pellet sands; ES – Eolian silt.
955 Eolian events (MS and ES) are clearly individualized, as are chernozems (IHS) and pellet sands
956 (PS).
957
958 Fig. 6. Dating of DV soil complexes, via correlations with several well-dated records, over the
959 60–120 kyr BP interval. Left: observed DV stratigraphy; middle: mean position of the DV
960 Optical Stimulated Luminescence (OSL) dates in the Greenland NGRIP $\delta^{18}O$ stratigraphy
961 (Andersen, et al., 2004); and right: comparison between the NGRIP (Andersen, et al., 2004) and
962 the Chinese speleothem $\delta^{18}O$ stratigraphies from the Hulu and Sangbao caves (Wang, et al.,
963 2008, Wang, et al., 2001).
964
965 Fig. 7. Correlation between DV soil complexes and several well-dated isotopic records. The
966 latter are shown, from left to right, as the three Greenland records of NGRIP $\delta^{18}O$ (Andersen, et
967 al., 2004), GRIP $\delta^{18}O$ and the GRIP dust record (Johnsen, et al., 2001); and the $\delta^{18}O$ from
968 NALPS speleothems (Boch, et al., 2011). Indication of Greenland interstadials (Rousseau, et al.,
969 2006) and of North Atlantic cold events from (McManus, et al., 1994).
970
971 Fig. 8. Maps of geopotential height anomalies at 500 hPa that show the onset, evolution and
972 collapse of the blocking structure that occurred over Eastern North Atlantic and Western Europe

973 in late 2011 and early 2012. Panels are organized from left to right and top to bottom
974 (November 2011 to April 2012; negative anomalies in cold colors and positive ones in warm
975 colors, while the contour lines indicate isopleths of the full-field climatology. Monthly
976 geopotential height data from the reanalysis of the U.S. National Centers for Environmental
977 Prediction (NCEP); see data library of the International Research Institute for Climate and
978 Society (IRI) at
979 http://iridl.ldeo.columbia.edu/maproom/.Global/.Atm_Circulation/.Monthly_Std_Height.html.
980 The shading for the anomalies starts at ±1 standard deviation, and the color contour interval is
981 0.5 standard deviation. The contour interval for the climatology is 20 gpm.
982

Figure1

Click here to download high resolution image

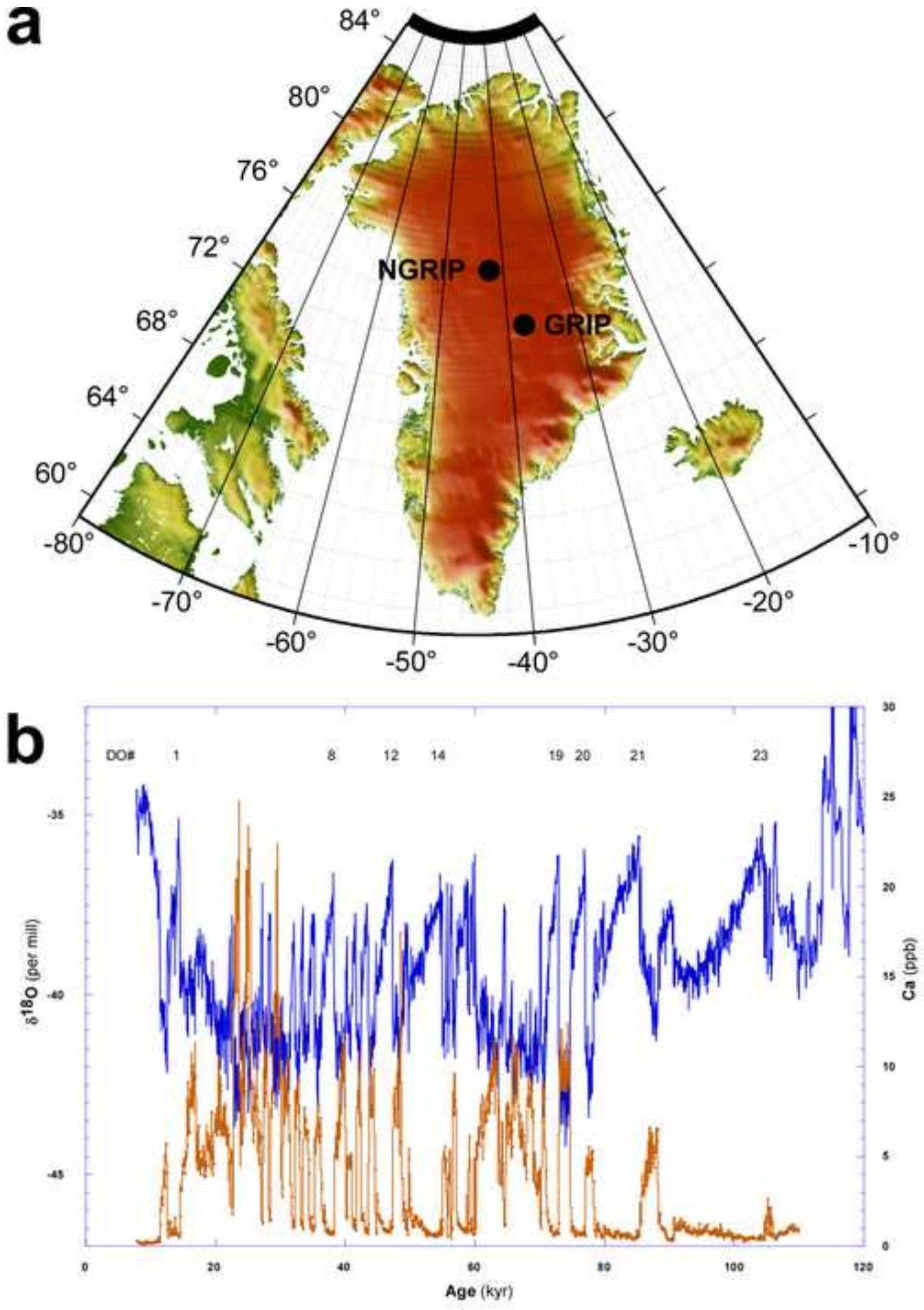

Figure2

Click here to download high resolution image

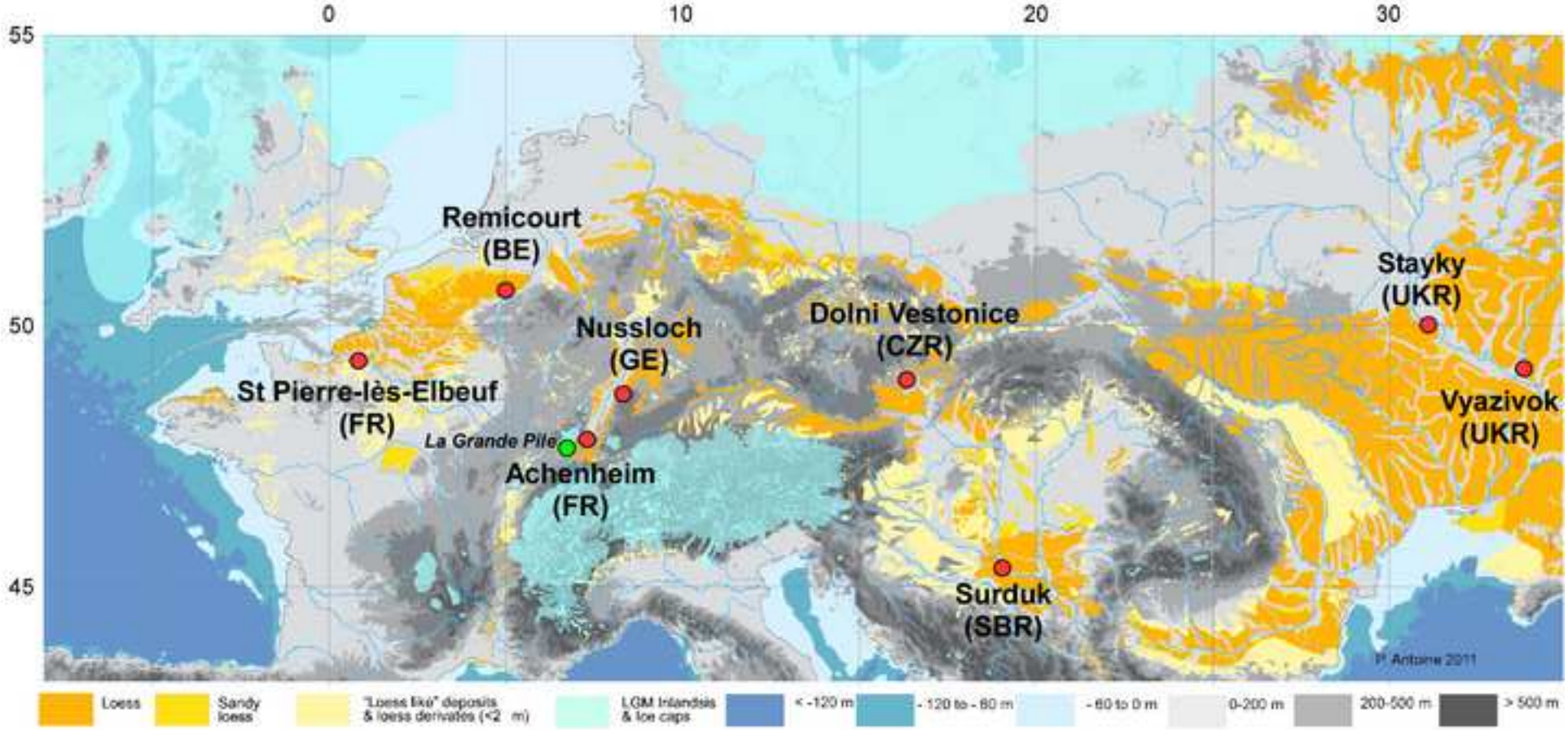

Figure3

Click here to download high resolution image

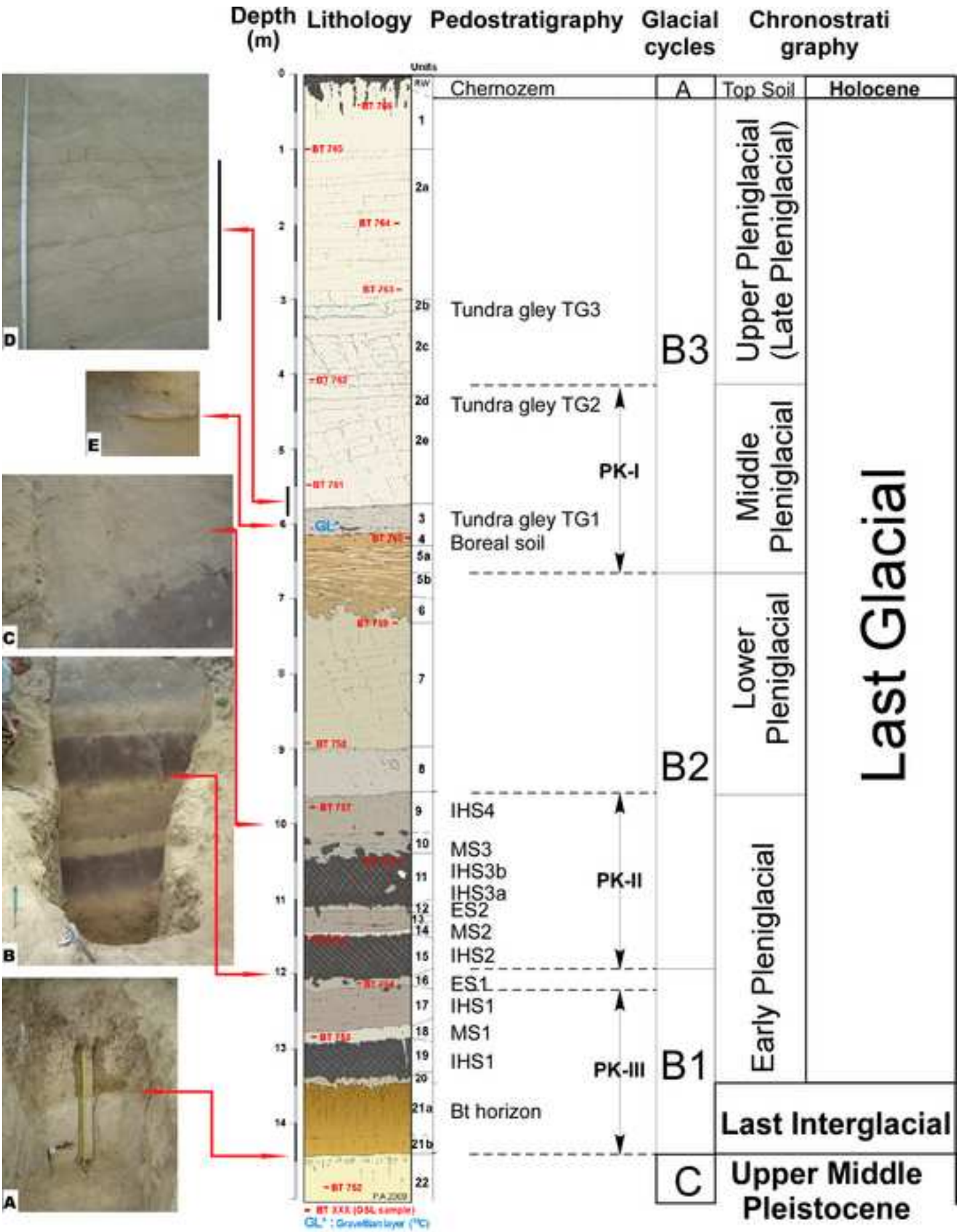

Figure4

Click here to download high resolution image

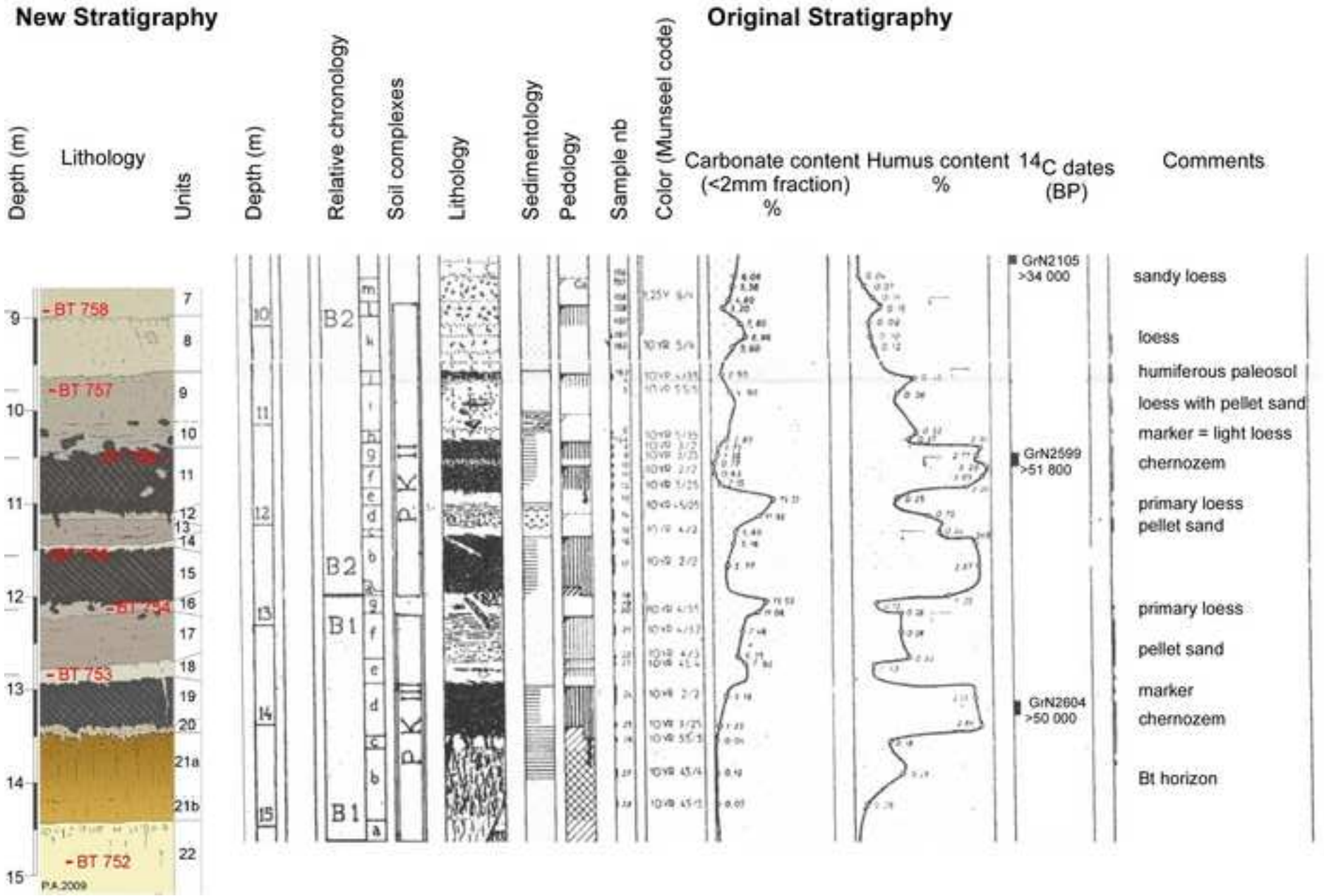

Figure5

Click here to download high resolution image

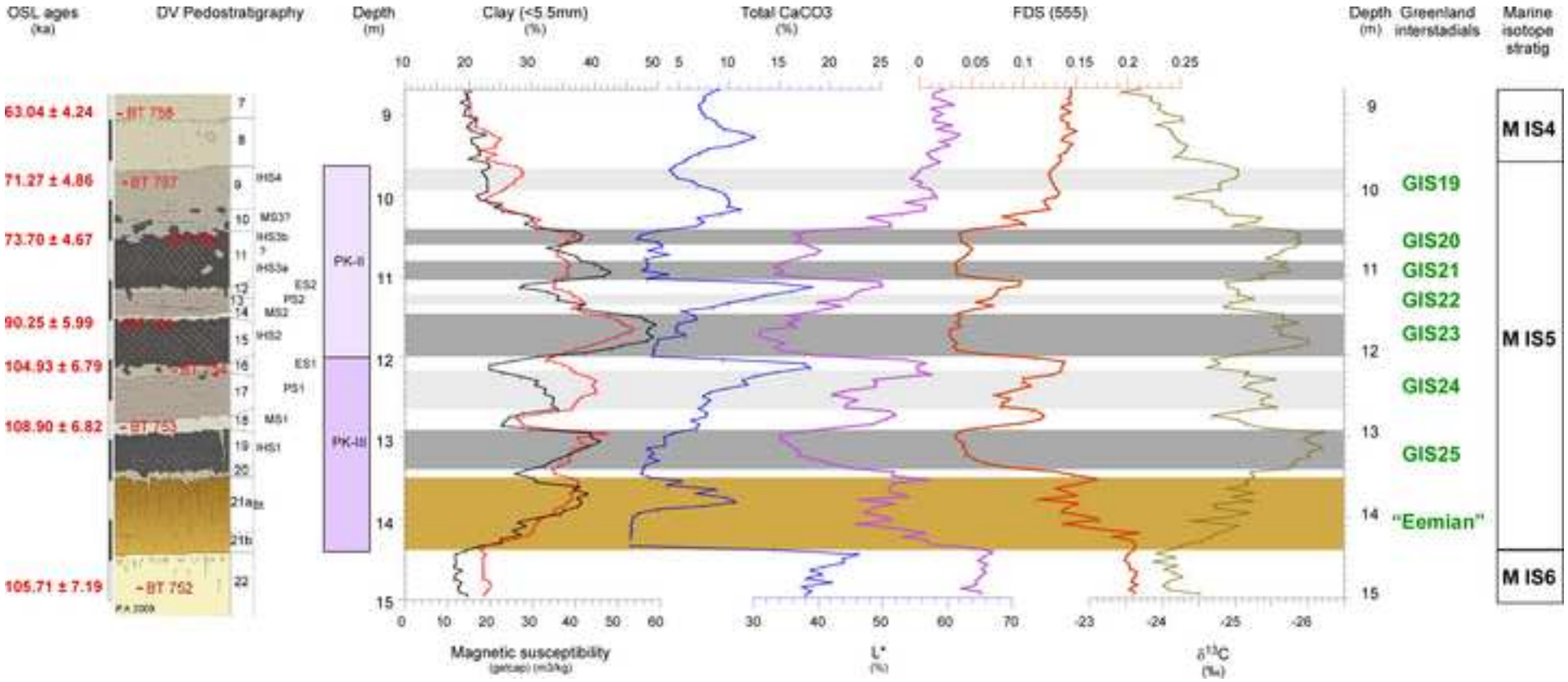

Figure6

Click here to download high resolution image

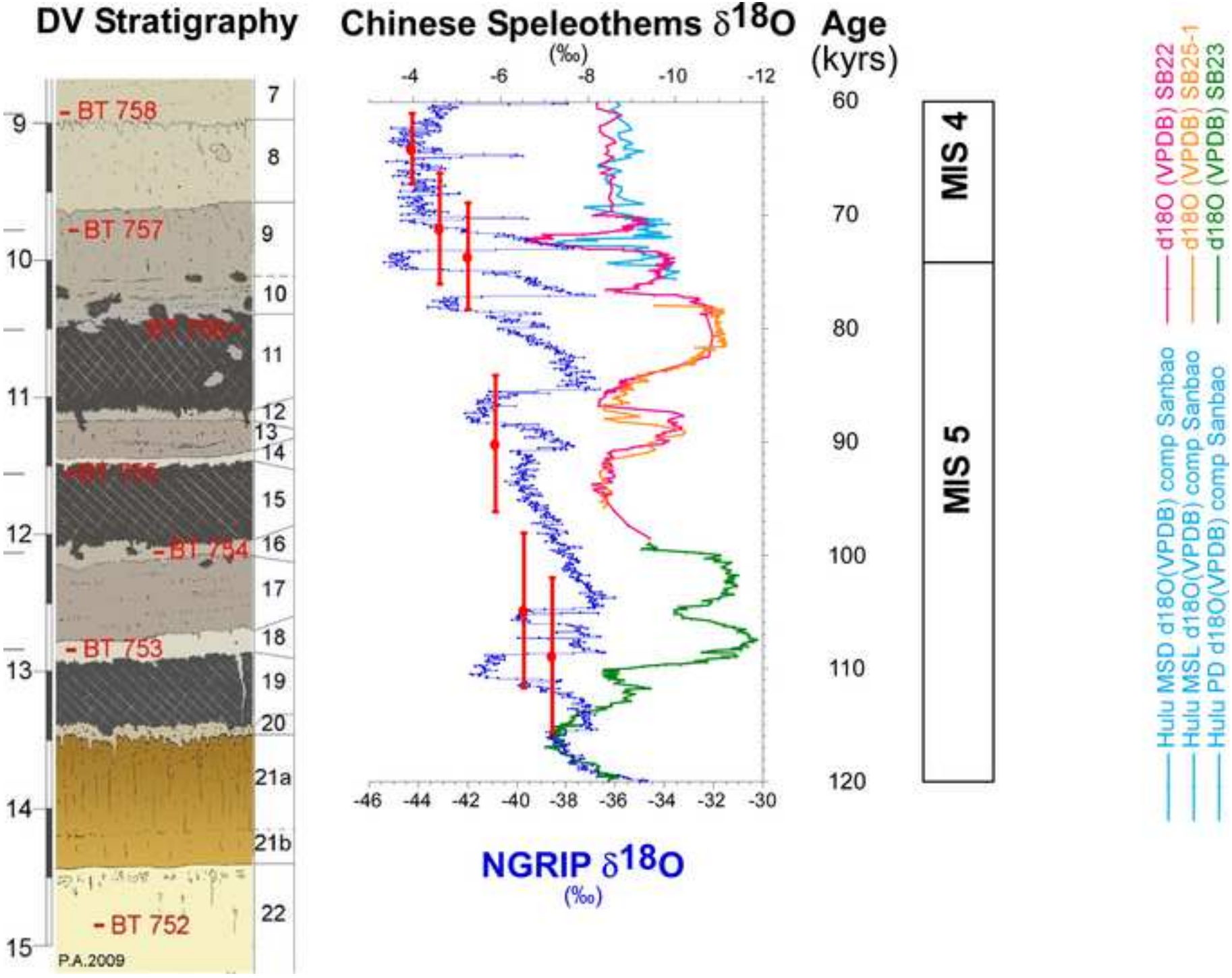

Figure7

Click here to download high resolution image

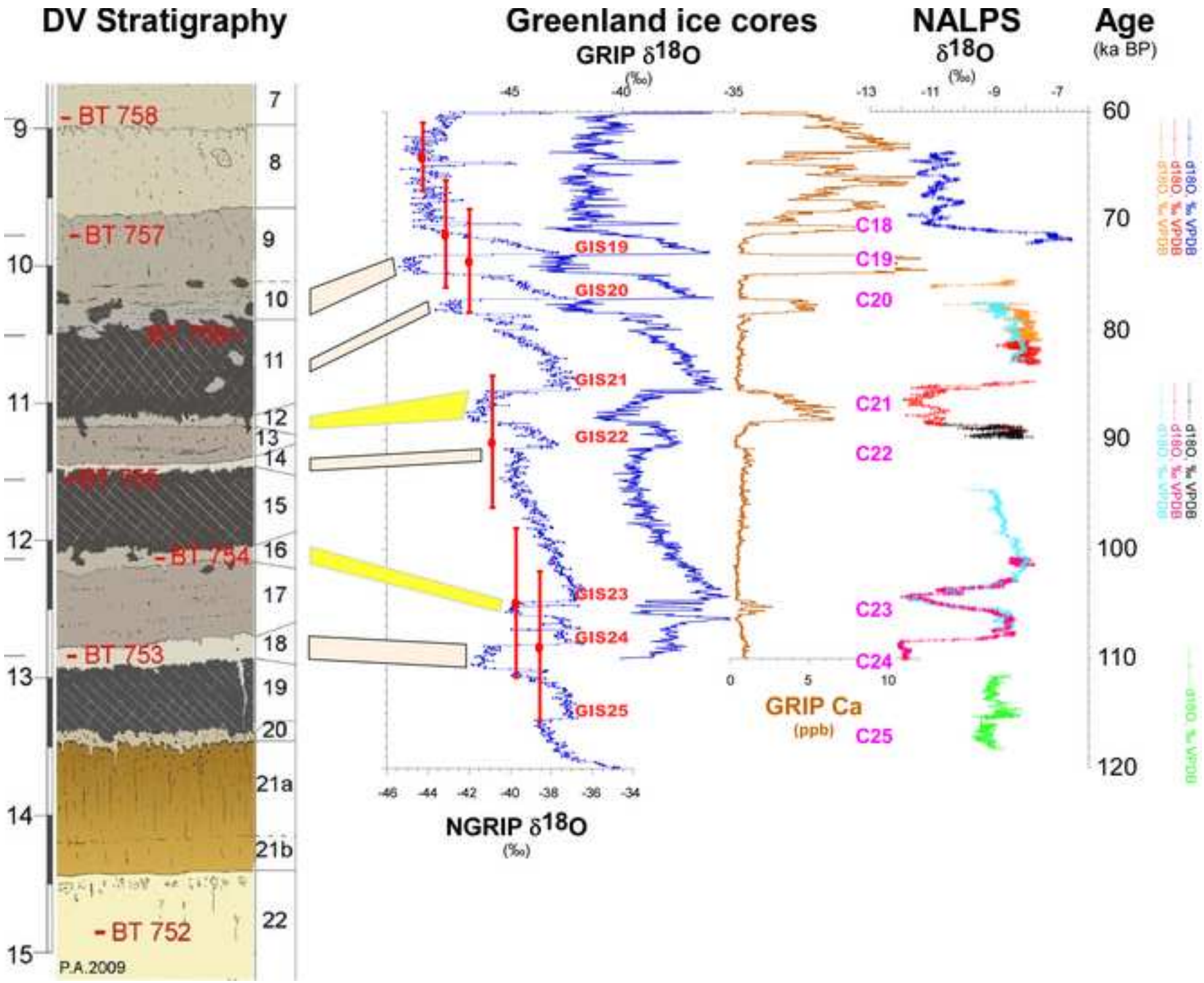

Figure8

Click here to download high resolution image